Geological Field Trips and Maps

2026
Vol. 18 (1.3)

Morphological analysis of Hala crater, a floor fractured crater located within Gorgonum Chaos Basin, Terra Sirenum, Mars

https://doi.org/10.3301/GFT.2026.03

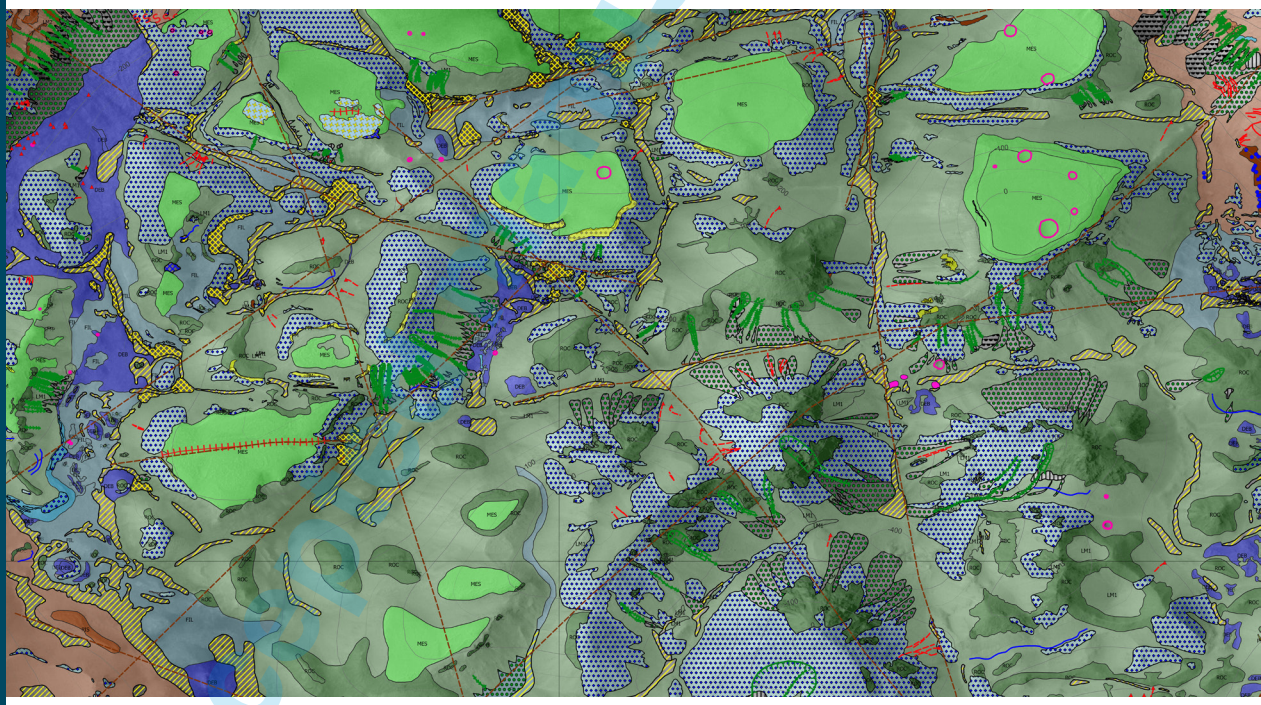

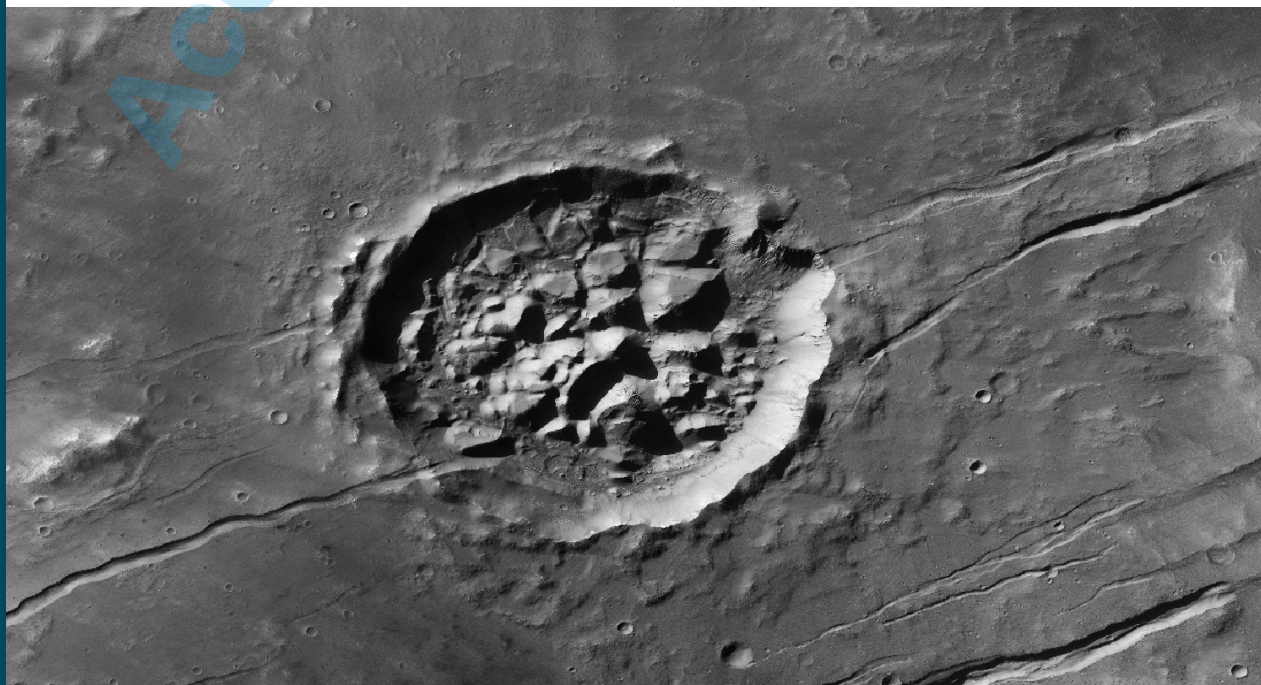

SOCIETÀ GEOLOGICA ITALIANA ETS
FONDATA NEL 1881 - ENTE MORALE R. D. 17 OTTOBRE 1885

ISPRA
Istituto Superiore per la Protezione e la Ricerca Ambientale

Sistema Nazionale per la Protezione dell'Ambiente

Geological Field Trips and Maps

Periodico semestrale del Servizio Geologico d'Italia - ISPRA e della Società Geologica Italiana ETS
Geol. F. Trips Maps, Vol. **18** No.1.3 (2026), 22 pp., 19 figs., 2 tabs. (https://doi.org/10.3301/GFT.2026.03)

Morphological analysis of Hala crater, a floor fractured crater located within Gorgonum Chaos Basin, Terra Sirenum, Mars

Silvia Bertoli[1], Matteo Massironi[2], Maria Cristina Salvatore[3], Carlo Baroni[3], Gabriele Cremonese[1], Maurizio Pajola[1], Ernst Hauber[4], Giovanni Munaretto[1] & Adriano Tullo[1]

[1] INAF, Osservatorio Astronomico di Padova, Padova, Italy. [2] Department of Geological Sciences, University of Padova, Padova, Italy. [3] Department of Earth Sciences, University of Pisa, Pisa, Italy. [4] Institute of Planetary Research, DLR, Berlin, Germany.

SB, 0000-0003-2243-0485; MM, 0000-0002-7757-8818; MCS, 0000-0002-1590-7284;CB, 0000-0001-5905-4650; GC, 0000-0001-9021-1140; MP, 0000-0002-3144-1277;EH, 0000-0002-1375-304X; GM, 0000-0001-7904-2657;AT, 0000-0003-4292-7093.

Corresponding author e-mail address: silvia.bertoli@inaf.it

Cover
Above: ...
Below: ...

ISSN: 2038-4947 [online]

http://gftm.socgeol.it/

INDEX

ABSTRACT

Floor-Fractured Craters (FFCs) are complex impact structures characterized by fractures, mesas, and knobs on their floors. They appear extensively on Mars, exhibiting diverse morphologies indicative of multiple geological processes including tectonic, volcanic, glacial, and fluvial mechanisms. This study presents a high-resolution geomorphological analysis of Hala crater, an 18 km-diameter FFC located within the Gorgonum Chaos Basin, in Terra Sirenum. Utilizing high-resolution imagery from HiRISE, CaSSIS, and topographic data from HRSC-derived DTMs, we compile a geomorphological map at a scale of 1:25,000. Detailed morphometric analyses reveal the crater is anomalously shallow compared to neighbouring structures, implying significant infill processes possibly influenced by magmatic intrusion and localized uplift events. The alignment of fractures within the crater notably correlates with regional tectonic stresses from the Sirenum Fossae system, suggesting substantial structural control. Periglacial landforms further illustrate extensive modification by ice-related processes during the Amazonian.
Overall, our detailed geomorphological mapping highlights a complex interplay of impact-driven, tectonic, volcanic, and periglacial processes that have shaped the crater's interior. This analysis contributes to our understanding of the geological history of FFCs.

KEYWORDS: floor-fractured crater, cryosphere, tectonic, magmatic intrusion.

INTRODUCTION

Floor-Fractured Craters (FFCs) are impact craters characterized by the presence of fractures, mesas, and knobs on their floors. First identified on the Moon in the 1970s, these craters have been observed on multiple planetary bodies. Schultz (1976) conducted one of the earliest systematic studies, classifying lunar FFCs based on their morphological characteristics. Their frequent association with basaltic maria suggests a possible volcanic origin. On Mars, however, the formation mechanisms of FFCs appear more complex. A global survey using Viking and MOLA data (Korteniemi et al., 2006) revealed a widespread distribution, and several hypotheses even involving volatiles, namely ice and liquid water, were proposed to explain their fracturing processes. In particular glacial (Morris & Underwood, 1978; Pechmann, 1980; Hiesinger and Head, 2000), fluvial (Sato et al., 2010; Zegers et al., 2010), volcanic (Wichman & Schultz, 1996; Jozwiak et al., 2012; Luzzi et al. 2021), and tectonic processes (Smrekar et al., 2004; Hanna & Phillips, 2006) were alternatively proposed as shaping agents of these features. Given this diversity of possible mechanisms, it is likely that multiple geological processes interact to produce FFCs.
While several studies have focused on classifying FFCs in different Martian regions (Bamberg et al., 2014; Korteniemi et al., 2006; Sato et al., 2010; Montigny et al., 2022), detailed cartographic analyses of individual craters remain scarce (Bamberg et al., 2014). In this work, we present a high-resolution geomorphological map of Hala crater, an 18 km-diameter crater located within Gorgonum Chaos Basins, Eridania Basin, Terra Sirenum. This crater exhibits a blunt, degraded rim and a chaotic floor characterized by a polygonal fracture network that segments the surface into irregular blocks, some of which remain partially preserved. Our mapping integrates data from CTX (Malin et al., 2007), HiRISE (McEwen et al., 2007), CaSSIS (Thomas et al., 2017), and HRSC-derived DTMs (Jaumann et al., 2007) to systematically document the spatial distribution of fractures, mesas, and floor materials. By identifying and classifying different morphological units, we aim to build a dataset that will help evaluate the potential role of the different processes in the development of floor fractures. In particular, we seek to investigate the relative contributions of ice-related processes and tectonic activity in shaping the observed fracture patterns.

GEOLOGICAL CONTEXT

The Eridania basin (Fig. 1) consists of a series of interconnected, quasi-circular sub-basins, likely formed by ancient impact events and subsequently modified by volcanic activity and erosion in the early history of Mars (Pajola et al., 2016b). Its extent has been previously defined by the 1,100 m elevation contour that surrounds these sub-basins. Based on this topographic boundary, Irwin et al. (2004) inferred that the basin was once filled with water up to this level, as indicated by the origin of Ma'adim Vallis, a 3 km-wide outflow channel, at the same elevation. The absence of upstream tributaries suggests that Ma'adim Vallis formed at its full width, further supporting the hypothesis of a spillover event. A potential spillway at the edge of the basin reinforces the idea that the Eridania basin held a substantial body of water at the Noachian/Hesperian boundary. The unique hypsometry of the Eridania basin, as noted by Irwin et al. (2004), is characterized by an unusually concave topographic profile. This morphology suggests that the basin floor was protected by standing water or an ice-covered lake during the most intense period of erosive activity on Mars.
One of the key sub-basins, Gorgonum Chaos, is located in Terra Sirenum (Fig. 2A). It measures approximately 240 km in diameter, with a maximum depth of 400 m. The graben system of Sirenum Fossae, which extends radially from the Tharsis region, cuts through this basin from east to southwest (Wilson & Head, 2002). The floor of Gorgonum Chaos is dissected by numerous fluvial valleys and features irregular knobs and mesas, particularly in its northern and western regions (Wendt et al., 2013). Impact craters larger than 20 km in diameter in this region show significant erosion and are largely infilled with sediments (Capitan & Van De Wiel,

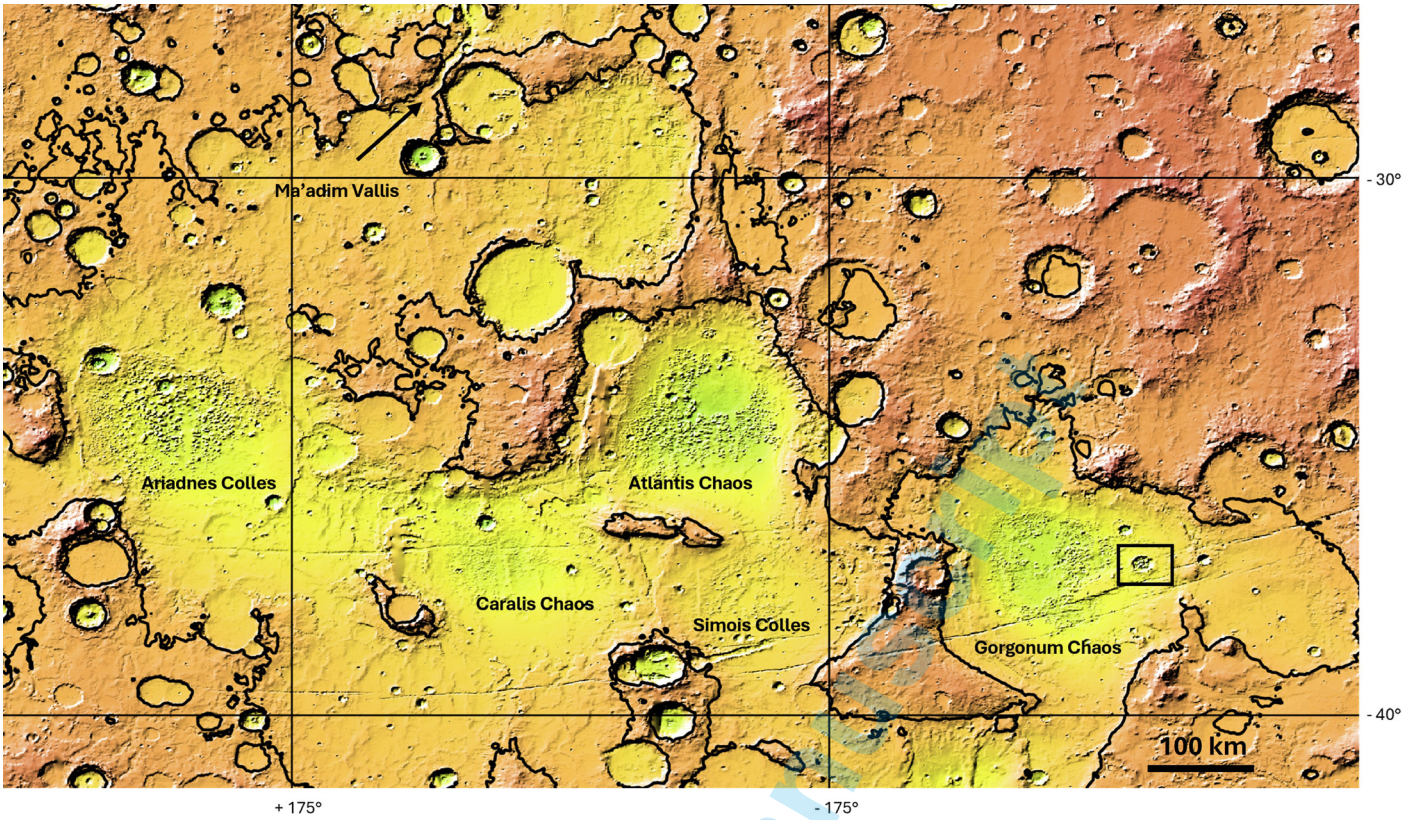

Fig. 1 - Eridania basin digital terrain model (128 pixel/degree) projected and color-coded from Mars Orbiter Laser Altimeter (MOLA). The black line indicates the 1100 contour line and the box highlighted Hala crater.

2011). According to Howard & Moore (2004), the absence of large impact craters superposing the flat basin floor suggests that it was once covered by an ice-sheeted paleolake. This hypothesis is further supported by the presence of light-toned materials, often associated with hydrated minerals or chlorides, which characterize the presumed paleolake floor (Adeli et al., 2015; Grant et al., 2010; Osterloo et al., 2010; Wendt et al., 2013; Pajola et al., 2016b). Using a crater production function (Ivanov, 2001) and absolute chronology models (Hartmann & Neukum, 2001), Michalski et al. (2017) estimated a minimum exposure age of 3.47 Ga for the Gorgonum deposits. These ages align with previous studies suggesting that the Eridania basin-forming impacts occurred more than 4 Ga ago, that a sea existed in the Late Noachian, and that resurfacing by subaerial volcanism took place in the Late Hesperian (Adeli et al., 2015).
The studied crater is located on the eastern wall of the Gorgonum Chaos basin (Fig. 2A).

DATA

Data Used

This study is based on data retrieved from the **Mars Orbital Data Explorer** of the Planetary Data System Geoscience Node (ODEMars) and the **Digital Terrain Model Reduced Data Record (DTMRDR)** catalogues of the Lunar and Planetary Laboratory (LPL). The data utilized are as resume in Table 1.

METHODS AND TECHNIQUES

The morphological mapping of Hala crater was carried out using CTX, HiRISE, and CaSSIS images. CTX data were used to analyze the surrounding landscape, while HiRISE and CaSSIS images supported detailed mapping. Mapping was conducted in QGIS 3.36.0 at a mapping scale of 1:2000 and using the equidistant cylindrical projection (also known as Plate Carrée, ID IAU_2015:49915) which introduces distortions toward the poles but is suitable for the study area.
The final map is presented at 1:25,000 scale (check the Supplementary material). The geomorphological mapping was carried out using both polygonal and linear shapefiles, depending on the nature of the features. Photogeological units and areal landforms, such as gully lobes, dune fields, and polygonal terrain, were mapped as polygons. Linear shapefiles were used to trace features such as gully channels, fractures, and tectonic lineaments. In some cases, features were also represented through hatch patterns to emphasize surface texture or distribution trends.

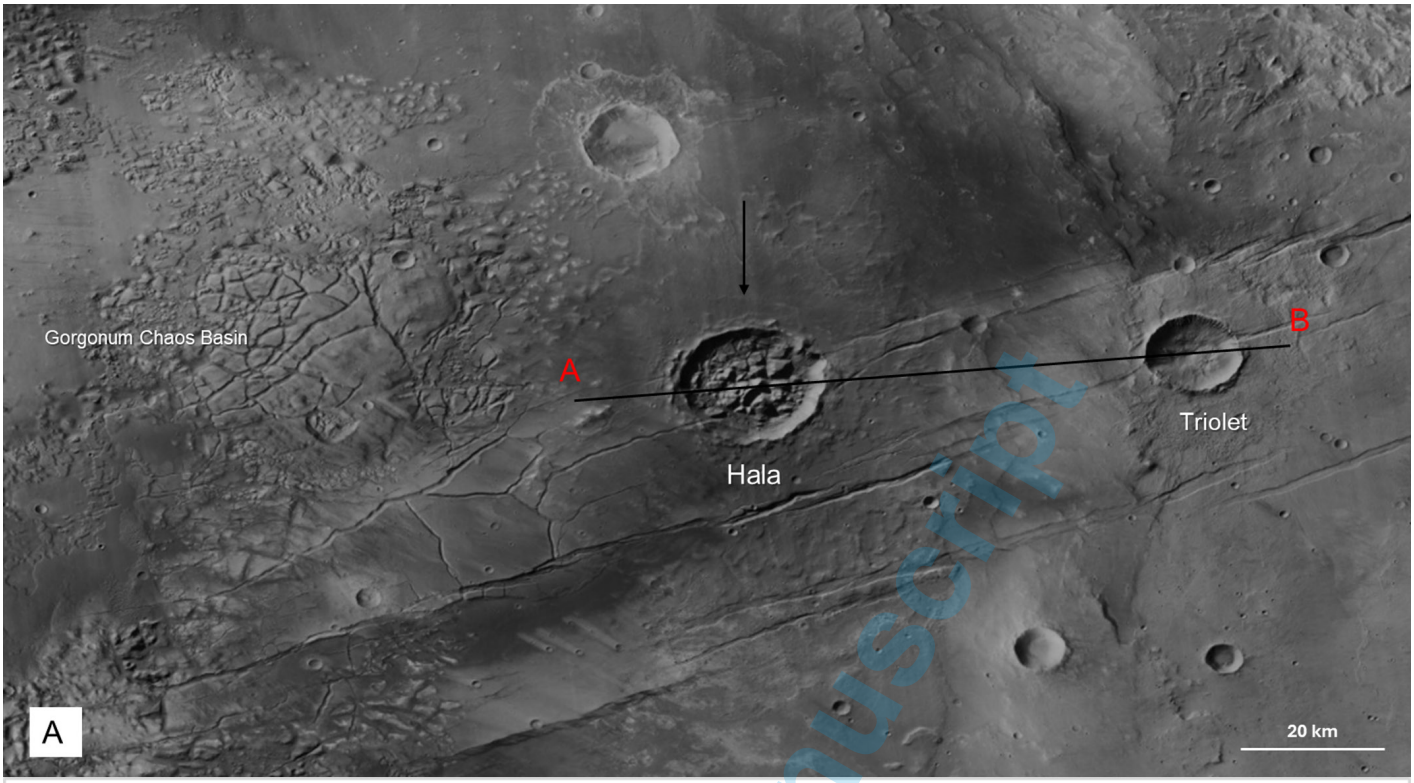

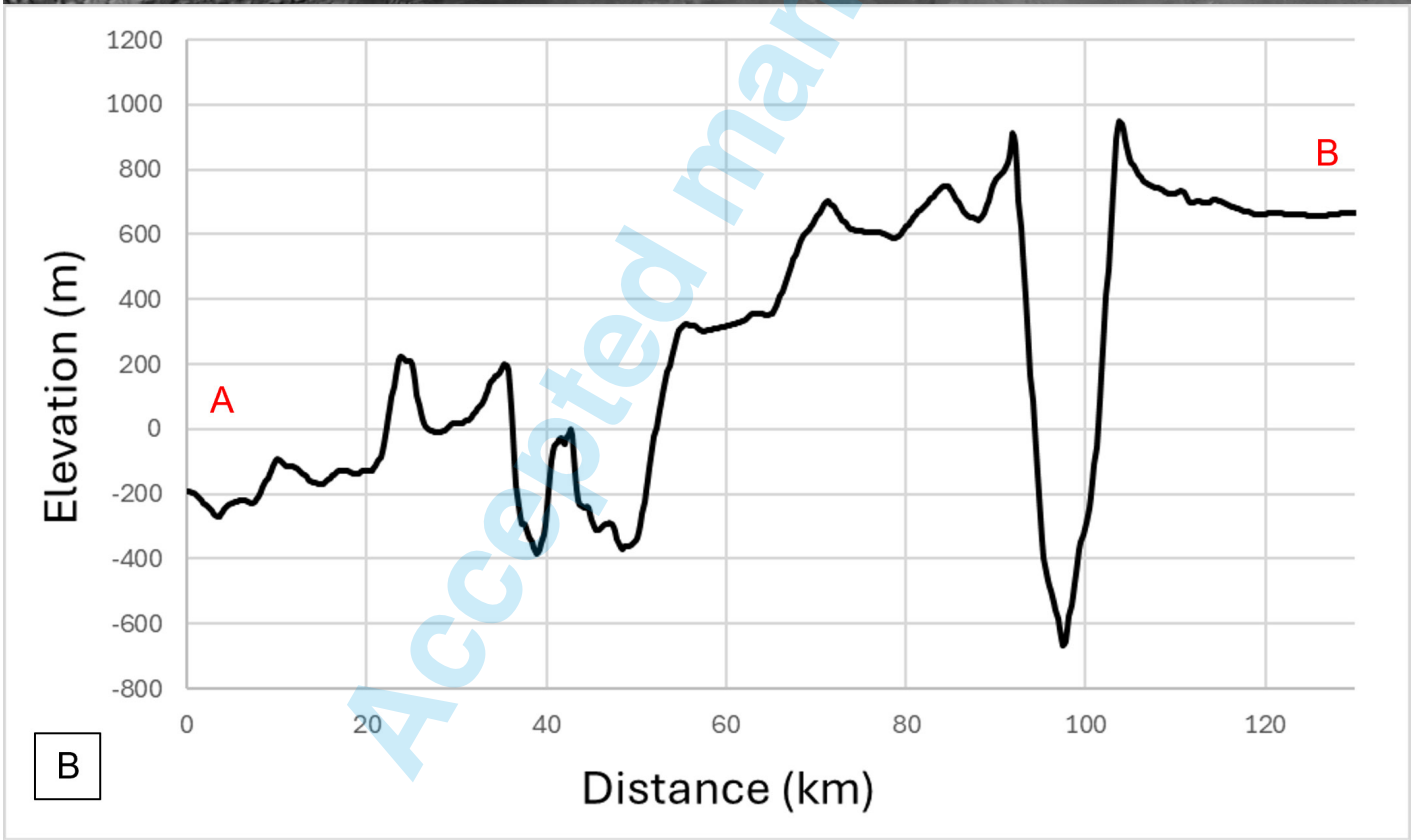

Fig. 2 - A) Location of the Hala crater within the Gorgonum Chaos Basin. The background imagery is derived from the CTX V1 Mosaic dataset (https://murray-lab.caltech.edu/CTX/). B) The topographic profile (3x vertical exaggeration) shows the inclination of the surface in which the crater has been formed. The black arrow indicates the studied crater, the other one on the right is the Triolet crater.

Table 1 - The table resumes the data used in this work (instrument, ID, source and the way in which we use them to analyse the crater).

Instrument	ID	Source	Use in this study
HRSC (High-Resolution Stereo Camera)	h0538_0000_da4	https://ode.rsl.wustl.edu/mars/	Topographic base for the analysis; generation of slope maps, elevation profiles, and mesa tilting measurements; extraction of crater morphometric parameters; support for structural interpretation.
CTX (Context Camera)	J08_048113_1425_XN_37S169W	https://ode.rsl.wustl.edu/mars/	Regional geomorphological context; mapping of surrounding terrain; first-order identification of floor units and aeolian features; base layer for figure mosaics.
HiRISE (High-Resolution Imaging Science Experiment)	PSP_007196_1425, PSP_002871_1425, ESP_036324_1425, ESP_024575_1425, ESP_048759_1425, ESP_048904_1425, PSP_007842_1425, PSP_007051_1425, ESP_057713_1425, ESP_048113_1425, ESP_048904_1425	https://ode.rsl.wustl.edu/mars/	Detailed geomorphological mapping; identification of small-scale landforms (gullies, polygons, pingo-like mounds, block fields, TARs); measurement of block sizes and fracture expression; cross-validation of unit boundaries.
CaSSIS (Colour and Stereo Surface Imaging System)	MY35_012371_220_0, MY35_011456_321_0, MY35_011543_321_0	https://observations.cassis.unibe.ch/	Color-based discrimination of units (albedo and spectral/color differences); support in distinguishing bright material (Bm) and platy material (Pm); confirmation of textural contrasts observed in CTX/HiRISE.

The units were identified through photointerpretation on the base of tone, texture, structure, size, and shape. The landforms were classified based on the identified or hypothesized morphogenetic agent. For features with indeterminate or complex origins, a neutral black color was used. The cartographic representation was partly inspired by terrestrial geomorphological legend (Campobasso et al., 2021) and partly modified to the specific requirements of this study, such as the impact features which have been mapped in pink and the not determinable features mapped in black. This approach ensured a clean, accurate, and interpretable map suitable for further landscape analysis.
The morphometrical analysis includes slope, elevation, object size, crater diameter, and crater depth measurements, as well as interpretation of lengths and orientation of linear features. Based on these data topographic cross-sections of the crater were generated, providing valuable stratigraphic insights. Rose diagrams of fractures and lineaments were produced using the Generic Mapping Tool, specifically the rose module (Wessel & Smith, 2013).

RESULTS

Topography and morphometric analysis

Hala crater appears shallower than the nearby Triolet crater (Fig. 2B), despite the latter being smaller in diameter. To assess the possibility of later infilling, we calculated the post-modification crater depth and morphometric parameters such as depth and width for the associate knobs and mesas (Fig. 3, Table 2, adapted from Bamberg et al., 2014).
According with Bamberg et al. (2014), for craters with diameters ranging from 7 to 100 km (in our case is 18 km), the following formula can be used to estimate the post-modification crater depth:

$$d_r = 0.357 \cdot D^{0.52}$$

where d_r is the crater depth from the rim crest and D is the crater diameter (both in kilometers). The depth of knobs (d_K) displays the height difference between crater rim and averaged knob elevation. The depth of fractures (d_F) is the difference between the average knob depth and the fractures' averaged measured incision. The observed crater depth (d_{Ob}) is the average between the d_K and the d_F. The thickness of infilling (T_I) is the difference between the d_r and d_K and it is the highest amount of infilling.

Table 2 - The table shows the results of the morphometric parameters of the crater.

Feature	Value (km)
Crater diameter (D)	18.0
Post-modification crater depth (d_r)	1.60
Crater depth (d_{Ob})	0.35
Depth of knobs (d_K)	0.43
Depth of fractures (d_F)	0.26
Thickness of infilling (T_I)	1.16

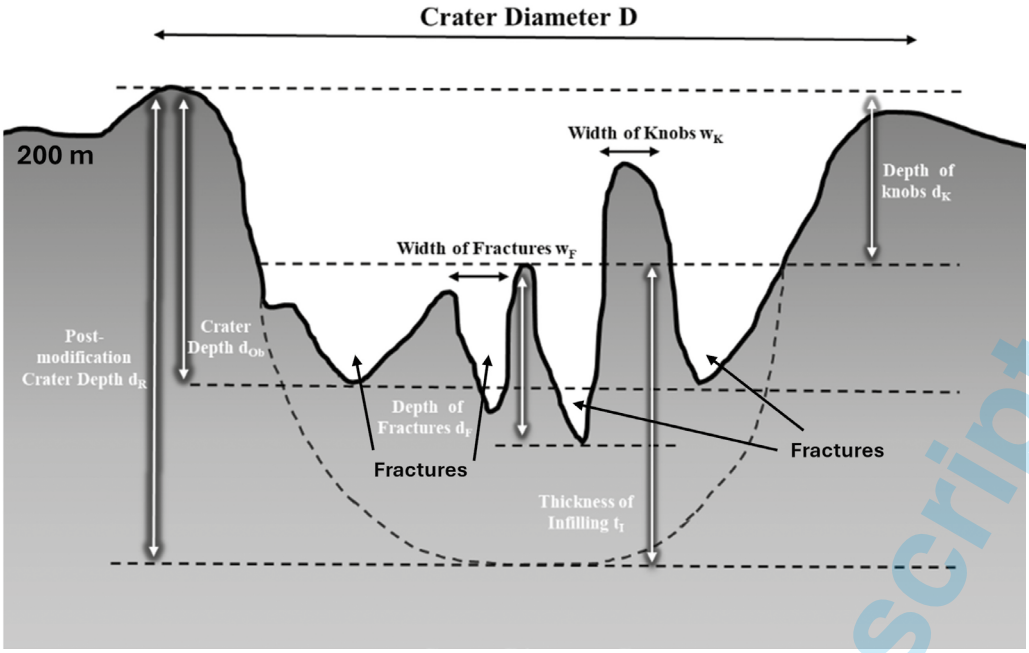

Fig. 3 - The image shows the profile of the studied FFC and the main features which have been measured. The fractures are indicated with arrows, and they separated the knobs.

BLOCKS AND MESAS FEATURES

The blocks in which the crater floor is divided can be classified into three types based on their shape. The first type, located in the northern part of the crater floor, consists of a flat-topped mesa with polygonal edges and a smooth texture. Furthermore, they are tilted toward the crater rim of about 3-4° (Fig. 4A-B). The second type, in the central area of the crater, resembles a knob, featuring a pointed summit, significant material deposition along its slopes, and less defined edges. The last type, located in the southeastern part of the crater floor, is characterized by small, lower, and closely spaced knobs.

CONTENT DESCRIPTION

Photogeological units

Based on the imagery data of HiRISE and CTX, we prepared a geomorphological map of Hala crater. The units are distinguished by their location within the crater in Wall Units and Floor Units. The Floor units group includes the Debris Bedrock (**Deb**) which is located mainly in the southern and eastern part of the floor, the Layered Unit (**Lay**) which occupies the southwestern part of the floor, the Filling unit (**Fil**), which represents the part of the crater floor with the filling material, the Mesa Unit (**Mes**), located in the top of the mesa, the Rocky unit (**Roc**) located under the Mes, the Loose material unit 1 (**Lm1**), which covers the slope of mesa, the bright polygonised material (**Bm**), which covers only a small portion of the floor and it is visible in the crater ejecta and the platy material (**Pm**), which occupies the rim of crater and the mesa scarps. The Wall Units are the Preimpact subsurface unit (**Pis**), widespread along the crater walls, and Loose material 2 (**Lm2**).

Floor units

Debris bedrock (**Deb**): this unit covers the southern, center and western part of the floor (Fig 5A). It is characterized by an alternance of light and dark tone of grey. The texture is rough and coarse, and the partial covering by the infilling material of the floor results in a spotted pattern. In this way the unit appears and disappears below the covering of the Lm2 unit. it is organized in small, rounded blocks (about 1 m in the major axis), which spread all over the floor.

Layered unit (**Lay**): the unit covers the south-eastern part of the floor. It presents a rough texture and a darker tone of grey with respect to the infilling material of the floor (Fig. 5B). The unit appears as hard rock, covered by aeolian material and retains some random impact craters. Fractures cut the rock mass into smaller blocks (Fig. 5C).

Filling Unit (**Fil**) is located all over the floor of the craters (Fig. 5D). It appears with light grey tone, smooth texture, and organized along linear and parallel pattern. It partially covers Deb and Lay units.

Mesa Unit (**Mes**): this unit is located on the top of the mesas (Fig. 6A -B). It has a light grey tone and a rough texture. We can observe the presence of impact craters, loose material organized in small dunes, and some circular/elliptical structures organized in parallel pattern. The thickness of the unit is very small (no more than 1 m).

Rocky unit (**Roc**): this unit outcropped on the central and southern knobs and stratigraphically lies below the mesa

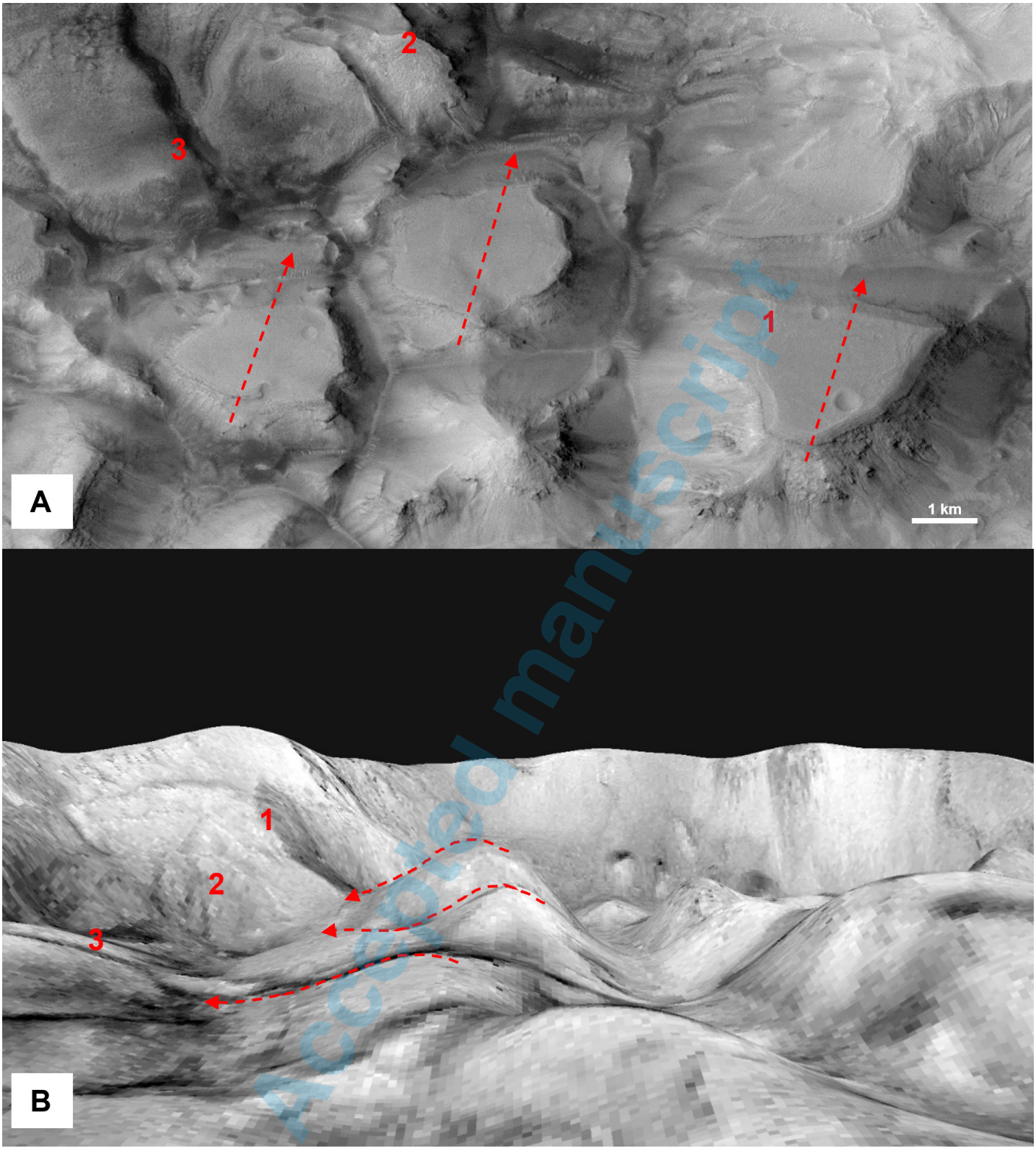

Fig. 4 - A) The image shows three mesas where dashed red lines indicate the direction of tilting. B) The image shows a HRSC 3D model of the crater. The dashed red lines outline the tilted mesa of the picture A. The vertical exaggeration of the 3D model is 3x.

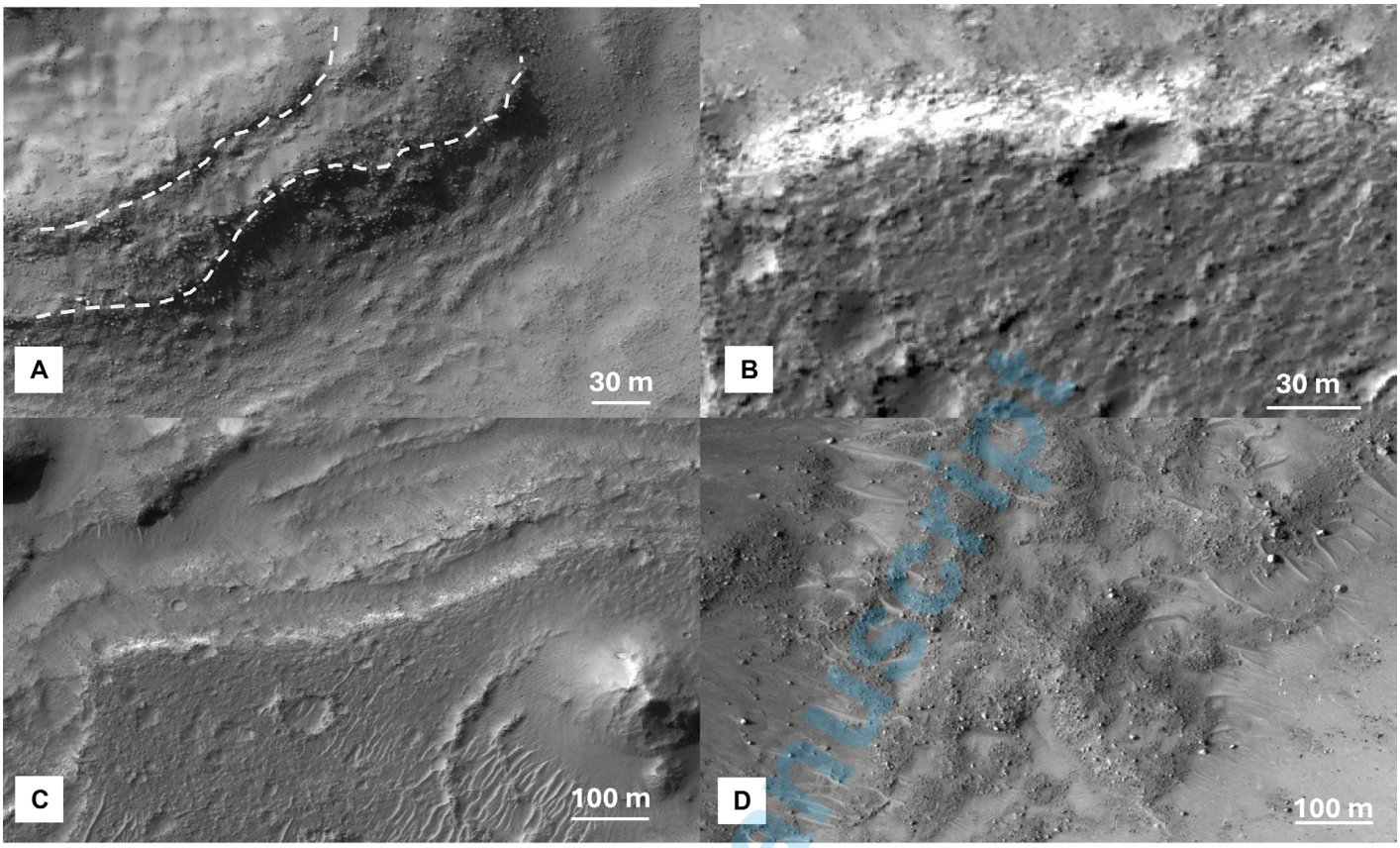

Fig. 5 - A) The image shows a portion of the Deb unit. It is layered and seems composed of blocks, which are visible at the HiRISE resolution. B) The Lay unit presents layering, and a structure more massive than the Deb unit. It is located close to the bottom of the crater wall, mainly in the southern and western sectors of the crater. C) Another view of the Lay unit, with the clear layering. The surface presents some impacts structures and aeolian landforms. D) The image shows the Fil unit, which covers the floor of craters. It presents alternation of fine graded material and some random blocks.

and platy material units. It has a dark tone of grey, and a rough texture. The outcrops appear as a solid rock (Fig. 6C), that under erosion produces rounded blocks accumulating at the crater floor.

Loose material 1 (**Lm1**) unit covers all the slope of the mesas. The material appears as light grey tone, with a smooth texture (Fig. 6D). Occasionally, the cover is uniform and smooth, likely composed of fine-grained material, while in some places it produces cones made up of coarser debris.

Platy material (**Pm**) unit is located on the rim of the crater and on the northern mesas' edges. It is characterised by dark to bright grey tones and organised in flat polygonal blocks (detail in Fig. 7A), varying in size from 3 to 8 metres along the longest axis. The unit emerges from beneath the Mesa unit, fractures into polygonal blocks that slide down and accumulate at the bottom of the mesa.

Bright material unit (**Bm**): this unit outcropped in the equator facing wall of the crater and randomly also on the ejecta. The portion inside the crater has a smooth texture and a light grey tone (Fig. 7B). The bright unit outside the crater have a polygonised surface and occupy mainly the western side of the outer rim.

Wall units

Preimpact subsurface unit (**Pis**) – This unit is located all along the inner slope of the crater, in particular in the equator facing wall. It presents a rough texture, dark tone of grey and it is organized mainly in leopard spots which follow the crater rim (Fig. 8A). The outcropping rock in situ appears as solid and angular and it is not present the blocky erosion, evident in the mesa bedrock.

Loose material 2 (**Lm2**) unit (Fig. 8B) is mainly located in the equator facing wall. The tone is made by an alternance of light and dark grey, the texture is smooth, and the material organized in talus cones.

MORPHOLOGY

Gravity induced landforms

Rockfall

Within the crater several rockfalls have occurred (Fig. 9A), resulting in the accumulation of coarse material at the

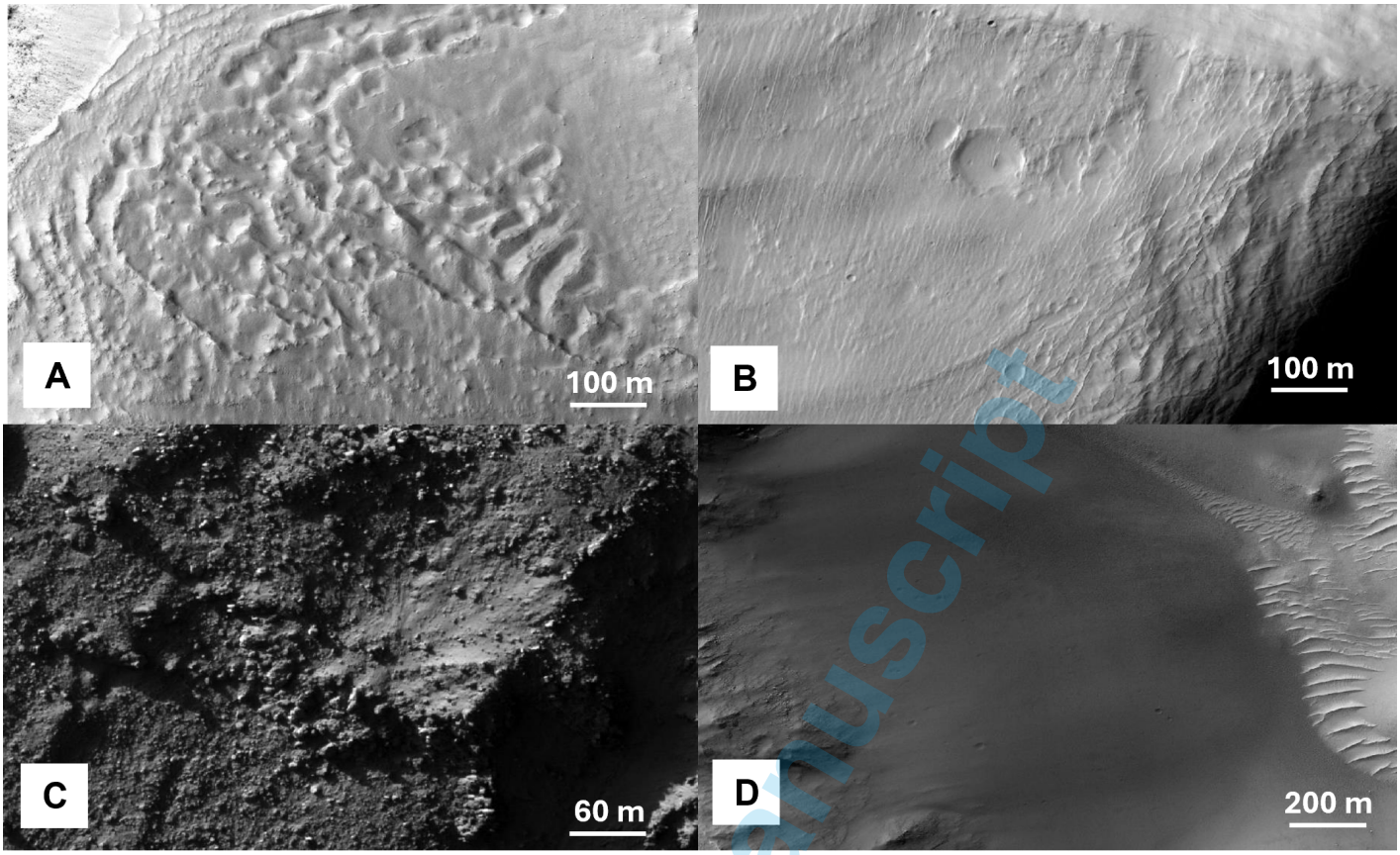

Fig. 6 - A) Mes unit which shows impact structures and aeolian landforms. B) The image shows one example of the Mes unit variability, which presents elongated and concave structures, filled with fine grained sediments. C) A detailed view of the Roc unit, which starting outcrop in the central blocks of the crater. D) The image shows Lm1 unit, which is located on the slope of blocks and mesa.

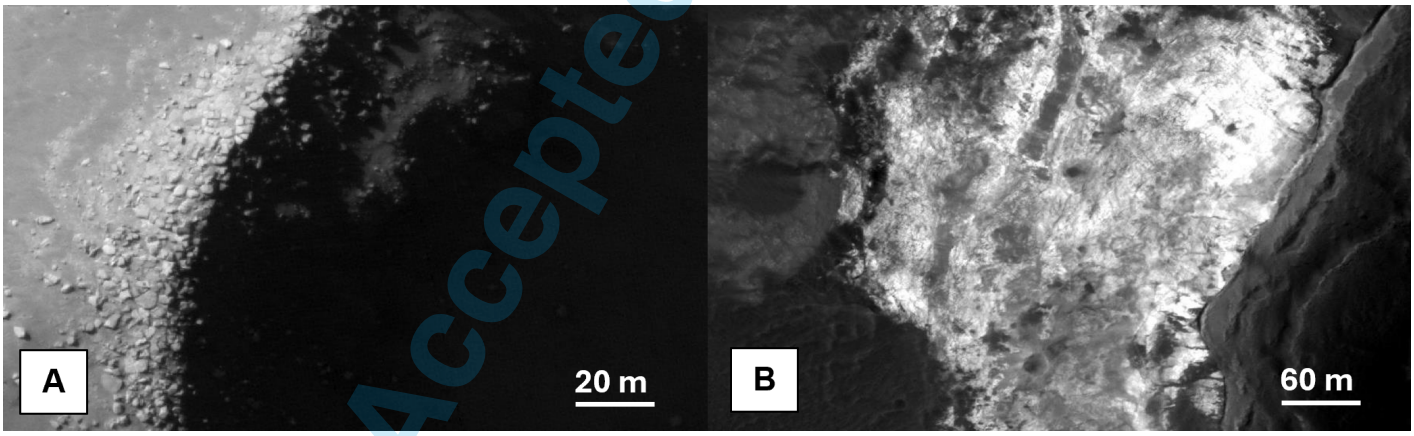

Fig. 7 - A) The image shows an example of Pm unit, which is located on the crater rim. It is also outcropped on the upper part of the northern mesa. B) A detailed view of the Bm unit, which presents a bright tone and a sort of polygonal texture. This part in particular is located on the proximal ejecta, but the unit outcropped also in the bottom of the crater wall, in the southern sector.

bottom of the slopes. The deposits are characterised by boulders of different size (an average of 3.5 m) located both along the crater walls and at the feet of the blocks constituting the chaotic floor. Where visible, we mapped the tracks left by fallen boulders that rolled, and bounced down the slopes

Deep-seated gravitational slope deformations (DGSSDs)

The DSGSDs are located in the south pole facing wall and on one of the central mesas (Fig. 9B). DSGSDs are a set of slow and complex gravity-driven deformational processes, involving entire slopes (or large portions of them) over long

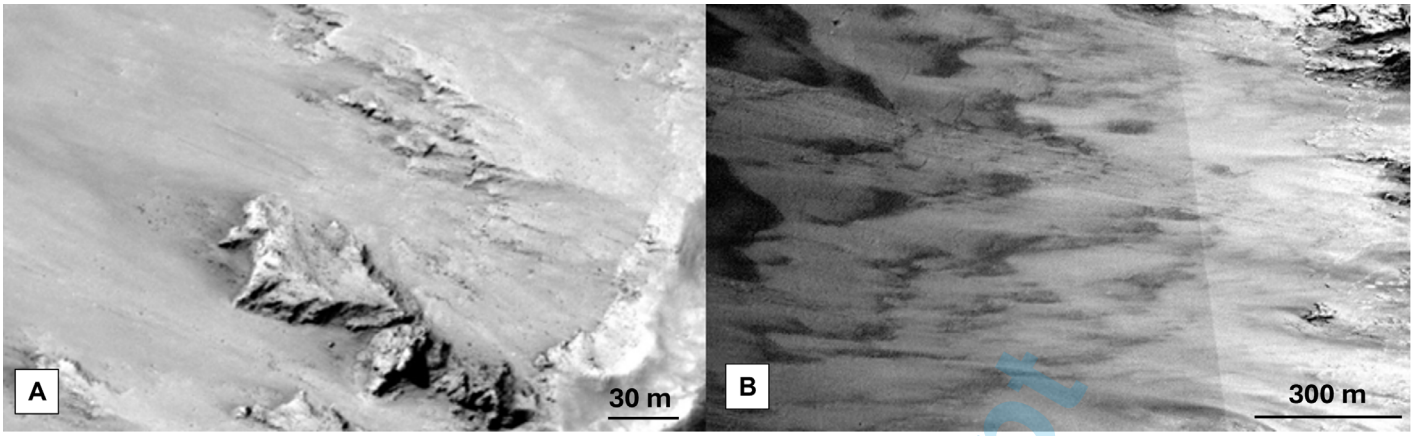

Fig. 8 - A) The image shows Pis unit which outcrops in the upper part of the crater wall. B) A close view of the Lm2 unit, which present an alternation of light and dark tone of grey.

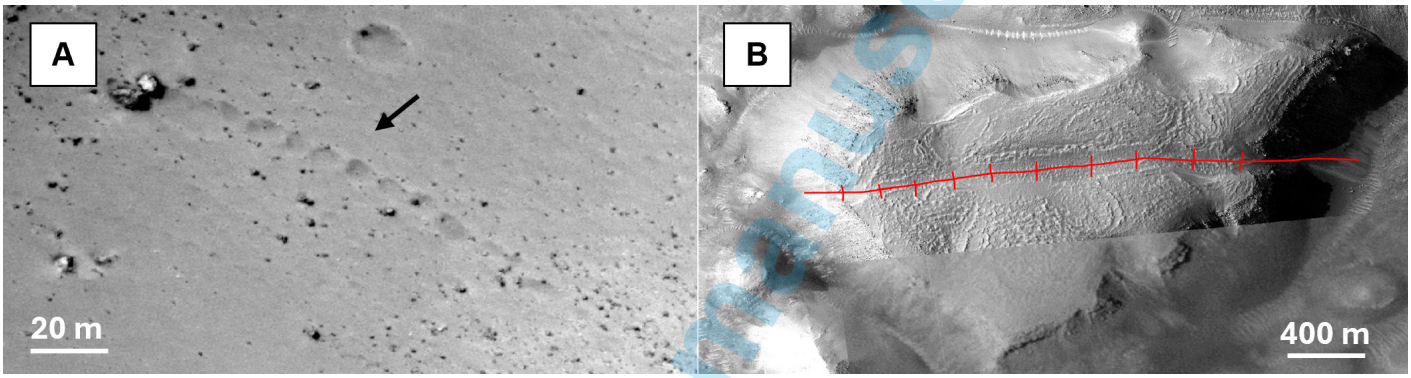

Fig. 9 - A) Falling track (indicated by the black arrow) of a boulder along the slope of a mesa (HiRISE ESP_048759_1425. B) The image shows the trench zone (red line) which identified a DSGSD located in a mesa within the crater (HiRISE PSP_002871_1425).

time intervals (Panek & Klimes, 2017; Agliardi & Crippa, 2022). Earth analogues are generally characterized by deformation rates on the order of millimetres per years, very small if compared with their enormous dimensions (Dramis and Sorriso-Valvo, 1994; Della Seta et al., 2017). DSGSDs of the crater are characterized by the typical morphological features such as double ridges, ridge-top depressions, trenches, and scarps (Pánek & Klimeš, 2017).

Aeolian landforms

Transversal Aeolian Ridges (TARs)

The crater floor fractures are infilled by fine grained filling material organised in linear structures, parallel to each other, which can be considered as Transversal Aeolian Ridges (TARs, Balme et al., 2008), (Fig. 10). They vary in size, with an average length of about 200 metres and width on the order of 40 metres and are all oriented SW-NE. Often the parallel arrangement gives way to sinuous and more complex shapes derived from the coalescence of several dunes, due to interference between them. The DEM available does not have adequate resolution to allow us to detect the individual dunes in 3D and the lighting conditions make it difficult to distinguish the upwind and downwind side. In places they present in the south-eastern side transversal dune arranged linearly along the development of the dune.

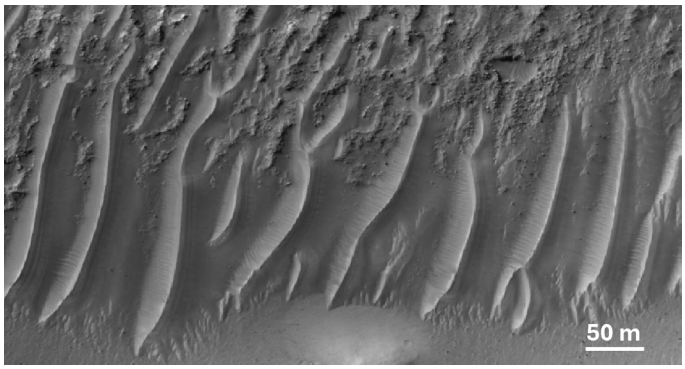

Fig. 10 - TARs in the southern part of the crater, which intersect the debris bedrock unit (CTX J08_048113_1425_XN_37S169W).

Periglacial landforms

Polygonal terrain

Polygonal patterned ground (Fig. 11) is observed along the outer rim of the crater. Each polygon exhibits well-defined quadrilateral shapes and a low surficial albedo. These features are consistent with thermal contraction polygons (Levy et al., 2009). since the crater's latitude is consistent with the presence of sufficient ground ice to cement permafrost (Mellon et al., 2004), as well as with models predicting the distribution of seasonal thermal stresses sufficient to induce thermal contraction cracking (Mellon et al., 2008). The variable polygons size may be attributed to the varying intensity of thermal contraction and the distribution of exploitable defects within the subsurface (Plug & Werner, 2001).

Block fields

Block fields are observed along the crater rim, on the rims of the mesa-type structures in the central part of the crater, and near other minor escarpments (Fig. 12A). The individual blocks exhibit angular margins, are generally piled up, and in some areas appear remobilised, forming extensive block sheets. Their sizes range from a few meters to several decameters, and they can either form extensive fields or be concentrated along the edges of the escarpments.

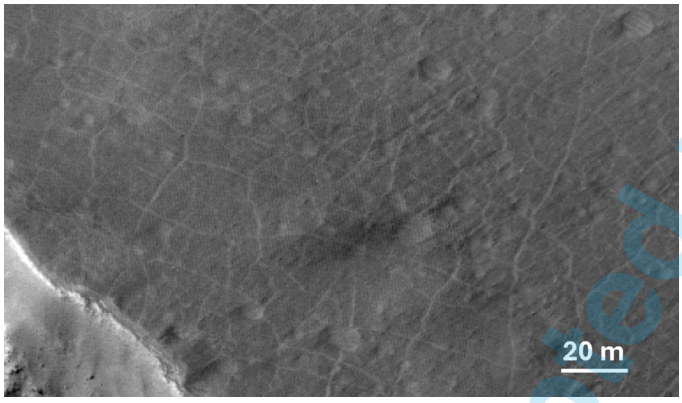

Fig. 11 - Detail of the polygonal terrain. (HiRISE PSP_007196_1425).

Protalus rampart

We mapped several elongated structures, referred to as protalus ramparts (Hedding et al., 2010; Hauber et al., 2011), distributed along the slope and exhibiting arcuate or irregular morphologies. These convex elongated landforms (Fig. 12B) occur along the walls of the central blocks oriented towards the south pole.

Pingo - like

Along the north-eastern sector of the crater wall, facing towards the south pole, convex circular structures with an average diameter of about 20 metres are exposed. These features, interpreted as pingos, are characterised at their summit by a central depression (Fig. 13A-B), bordered by small escarpments.

Erosional and depositional landforms - Gully-system

Detachment niches (Alcove)

Under the name detachment niches, we mapped all features of varying size located along the inner rim of the crater (especially in the sector facing the south pole) and along the slopes bordering the central blocks (mesa) (Fig. 14A). These features are erosional landforms attributable either to deepening of the incisions or to regressive erosion/ retreatment of the headward that pervasively affects the northern slopes.

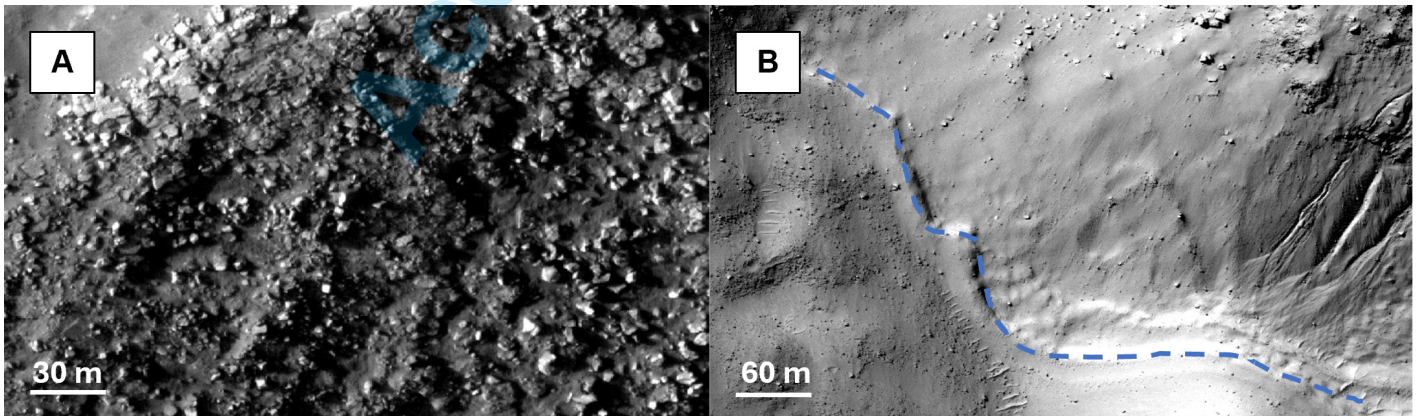

Fig. 12- A) A detail image of the block field on the western edge of the crater (HiRISE ESP_048759_1425). B) Protalus rampart at the bottom of mesa's slope (highlighted in blue dashed line, HiRISE PSP_002871_1425).

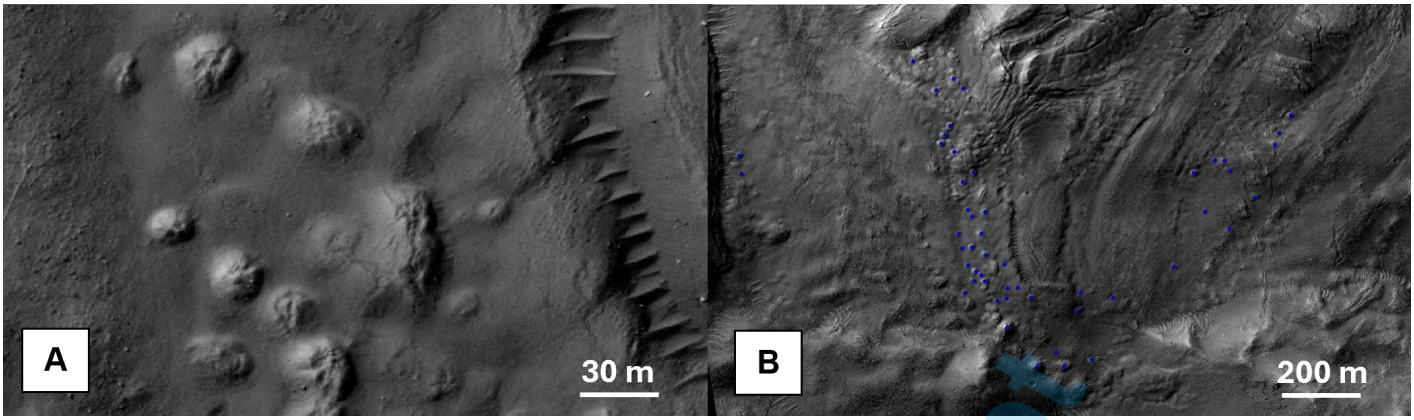

Fig. 13 A) The pingo-like landforms in detail, which present the typical depressed top (HiRISE PSP_007196_1425) B) Blue dots indicate the location of the pingo-like structures. They appear to be arranged in linear clusters oriented parallel to the local slope, indicating that their formation preferentially occurs along specific slope-aligned pathways, possibly controlled by pre-existing fractures or variations in subsurface permeability. (HiRISE PSP_007196_1425).

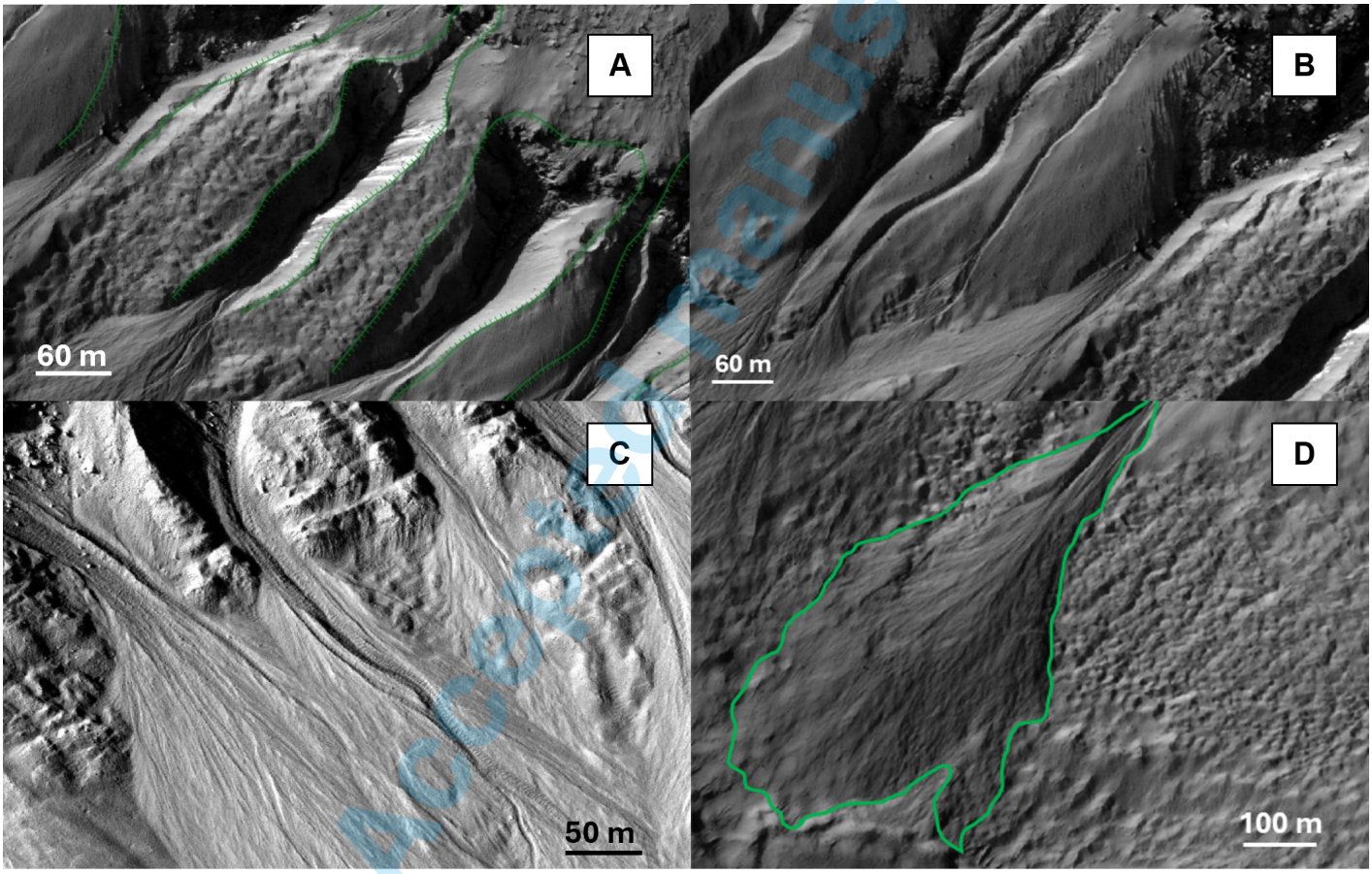

Fig. 14 - A) The image shows the alcoves located in the north-easter crater wall. B) The first type of channels identified within the crater, which recall classic structures of gullies. C) A detailed view of the second type of channels. They present a more complex history of reactivation, which form terraces at different level. D) One example of complex lobe located in the northern slope, associated with first type of channel.

Channel

Linear structures depart from the detachment niches, branching out along the slope. These channels are always located on the inner walls of the crater and the walls of the central blocks exposed towards the south pole. From a morphological point of view, we can distinguish two types of channels. The first type is the classic incision, characterised by embankments of variable length (Fig. 14B). The second type (Fig. 14C) concerns more

complex incisions, with possible terraced surfaces at its margins. The terraces indicate that there were several periods of channel incision and therefore several periods of activity. These types of channels are located in the south-east-facing walls in the north-western portion of the crater (HiRISE PSP_002871_1425). The material deposited is organized as single lobes or complex lobes (Fig. 14D). The latter in particular present structures which indicated more reactivation of the processes such as truncated channels and superimposed lobes.

Structural landforms

Fractures/faults

The lineaments mapped in this category are defined as alignments of point, linear or area elements that can be identified over extensive areas and attributed to geological processes. In Fig. 15A the main lineaments recognised in the study area are highlighted. They are traced by observing the alignments of different features such as gully incisions, truncated lobes, channels, crater rim and floor fractures. Patterns resulting from this particular distribution of gently curved or straight lines are common and have a structural significance. We measured the orientation of these lineaments with respect to the north, and we plotted the results in a rose diagram (Fig. 15B). The diagram highlighted that the longest fractures present within the crater have a predominance of ENE-WSW direction which is consistence with the direction of the Sirenum Fossae graben. However, the degree of dispersion of the lineaments as well as the polygonal pattern of the blocks indicate even local effect unrelated to regional tectonism but partially controlled by the structural pattern.

Poligenetics landforms

Weathered bedrock

Along the slopes of the crater facing the south pole, convex circular structures (~15 meters in diameter) have been observed (Fig. 16). These features are arranged longitudinally along the crater wall and are associated with the presence of gullies. Similar structures have also been identified on the south-facing walls of some central blocks within the crater floor. These landforms are interpreted as the result of weathering and exfoliation processes affecting pre-existing fractures in the substrate.

Longitudinal incision

Complex landforms include linear structures (Fig. 17) that are parallel to each other, narrow, and elongated along the slope, with an average length of ~10 meters and a width of ~1 meter. These features are particularly evident along the inner rim of the crater, on the south-facing slope near the pole, and on some south-facing walls of the central blocks. Morphologically, they closely resemble karren formations found in terrestrial karst environments (Bögli, 1960) or columnar basalts, which form as subaerial cooling structures in basaltic lava flows. However, we consider these analogues strictly morphological, not genetic. From a morphogenetic point of view, a periglacial origin is more consistent with their spatial distribution, slope-parallel alignment, and occurrence in mid-latitude terrains. Similar “sorted stripe”-like linear textures have been described in Hellas Planitia (Hubbard et al., 2011) and Promethei Terra (Bertoli et al., 2024), where they are interpreted as surface expressions of freeze–thaw processes affecting ice-rich regolith.

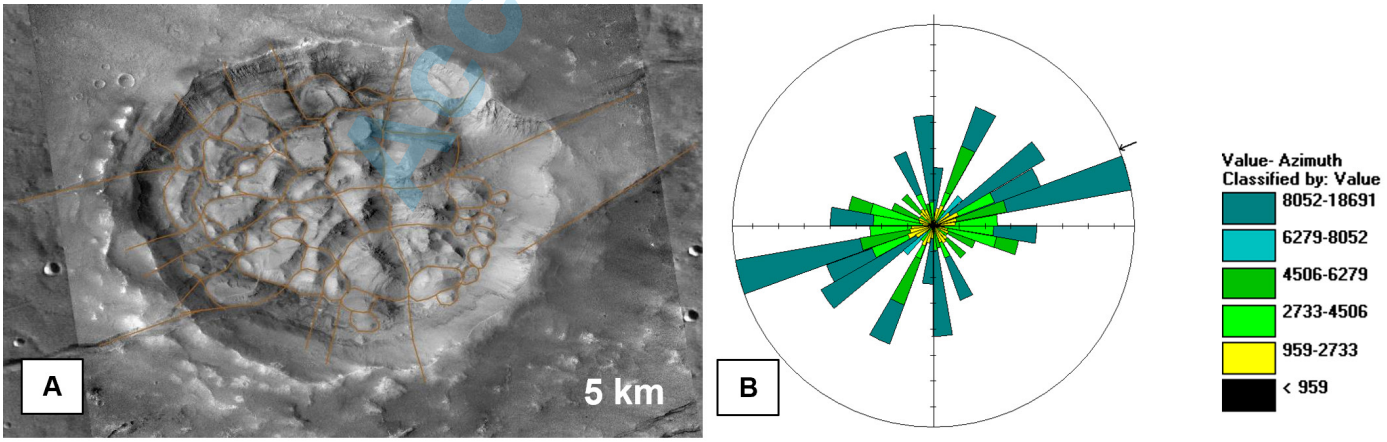

Fig. 15 - A) The image shows all the lineations recognized in the crater (CTX J08_048113_1425_XN_37S169W). B) The rose diagram shows the preferential direction of the fracture within the crater. The direction is weighted with the length (in meters).

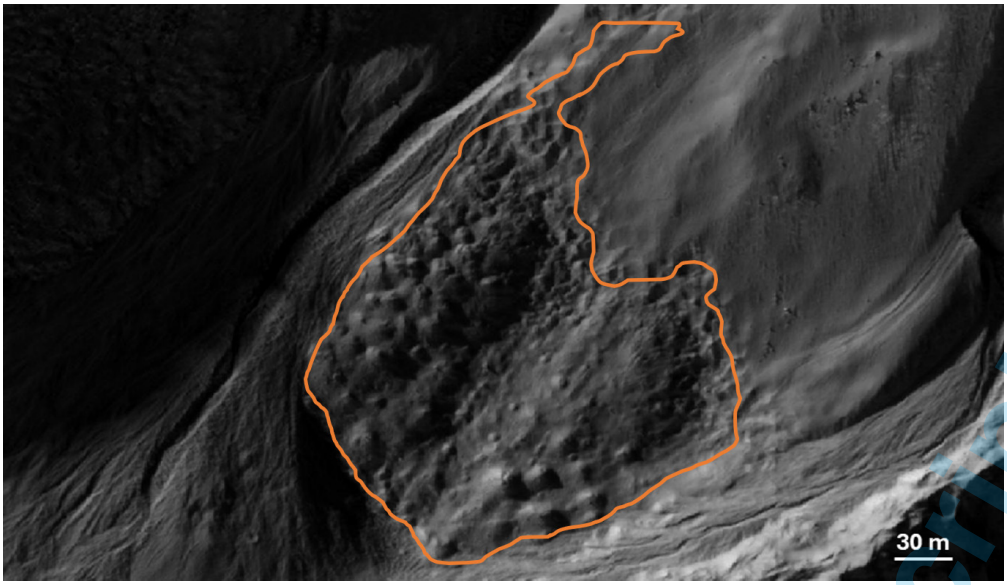

Fig. 16 - The image shows one example of the convex features, outcropping in the northern wall between two gullies. (HiRISE ESP_036324_1425).

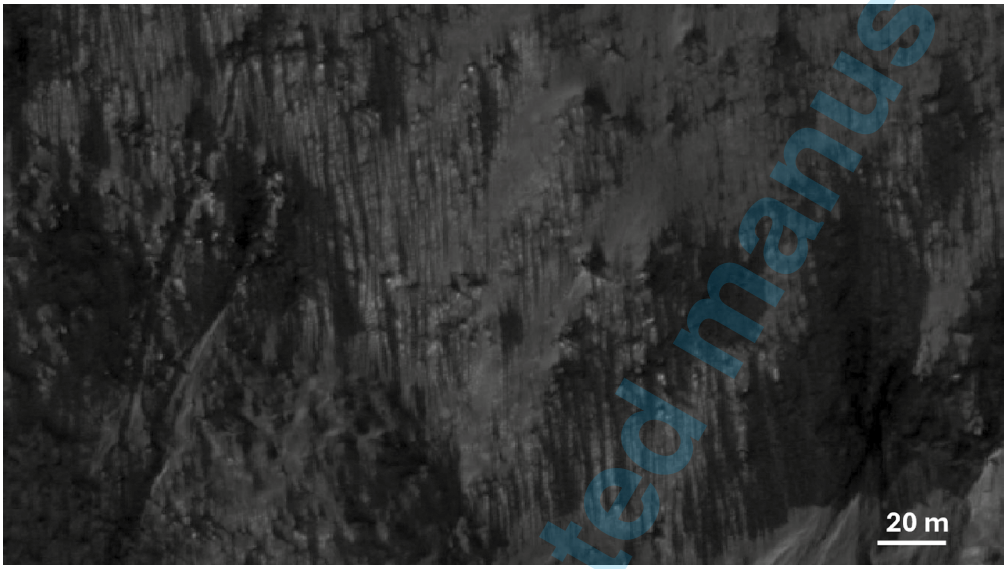

Fig. 17 - A) The image shows an example of the longitudinal incisions (northern wall, HiRISE ESP_036324_1425).

Recurrent Slope Linea

The polygenetic landforms also include dark features, primarily located along the west- and southwest-facing walls of the crater. These features range in length from 6 to 300 meters, with an average width of ~2 meters. In the literature, they have been described as Recurrent Slope Lineae (RSL; McEwen et al., 2011), which are relatively dark linear markings on steep slopes with low albedo, suggesting minimal coverage by bright dust. RSL typically originate from bedrock outcrops (McEwen et al., 2011). Fig. 18A-B illustrate the temporal evolution of these features on the southern wall, showing images taken ten years apart.

DISCUSSION

The geomorphological map presented in this study provides a comprehensive and detailed representation of the landforms within Hala crater, located in the southern hemisphere of Mars. This mapping effort is particularly significant, as high-resolution geomorphological maps of FFCs remain scarce in planetary studies. By integrating morphological, morphometric, and structural data, this work offers new insights into the complexity of the crater's interior and its post-impact evolution.

The map highlights the distribution and relationships among the main geomorphological units, differentiating between distinct materials and landforms that characterize the crater floor, central blocks, rim.

Starting from the impact itself, the presence of ice in the subsurface seems to have played an important role in the crater modification, probably right after the impact. In fact, the crater exhibits fluidized ejecta deposits (Fig. 19), classified as double-layered ejecta (DLE) deposits, which are commonly associated with impacts into volatile-rich substrates (Barlow et al., 2000). Several models suggest that these morphologies can form due to (i) impact into near-surface ice or volatile reservoirs (Carr et al., 1977;

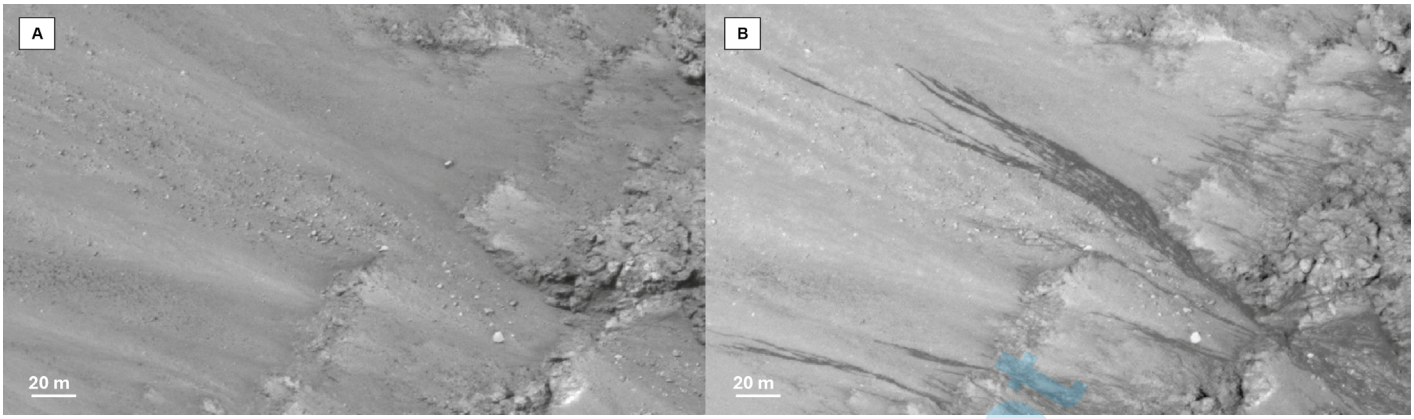

Fig. 18 - Comparison between two HiRISE showing the RSL activity. A) The image PSP_007196_1425, taken on 08 February 2008, shows the upper portion of the southern wall. B) The image ESP_057713_1425, taken on 18 November 2018, shows the same area of A, but we can clearly see that many RSL are present.

Mouginis-Mark, 1979), (ii) interaction between ejecta and the thin Martian atmosphere (Schultz & Gault, 1979), or (iii) a combination of both (Komatsu et al., 2007).

Being the crater located within the Gorgonum Basin, which is thought to be an ancient paleolake, we could hypothesize that the impact had happened when there were still volatiles inside the basin, either in form of liquid water or ice deposits. This possibility will be analysed in the following work to this paper, which it will provide crater counting analysis. Following a morphological point of view and the state of degradation of the ejecta blanket and seeing that the ejecta have been cut by the regional tectonic, we could hypothesize that the impact is pretty old, and thus the volatiles presence was highly probable.

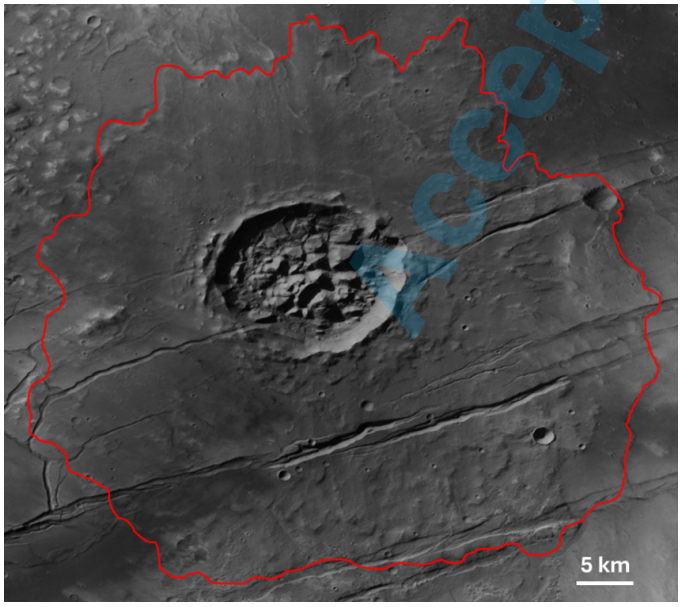

Fig. 19 - The ejecta blanket of the crater and its lobes are outlined in red.

The topographic analysis highlights a notable variation in the altimetry of the central blocks and unit distribution across the crater floor. Notably, four major units have been identified within the floor: (1) a mesa-forming unit (Mes unit), which retains evidence of stratified materials and presents clear indications of differential erosion; (2) a layered unit (Lay unit), which present stratified material located in the bottom of the crater slope, in the southern and western sector; (3) a platy unit (Pm unit), characterized by fragmented and disrupted materials; and (4) an exposed bedrock unit (Roc unit), associated with the highest knobs in the central and southern parts of the floor, where overlying deposits appear absent. This localized topographic prominence, combined with the absence of overlying deposits, suggests a possible uplift process that may be consistent with subtle doming (Walwer et al., 2021; Buczkowski et al., 2018). The mesa-forming unit, particularly in the northern sector of the crater, exhibits a systematic tilting of stratified layers toward the north, indicating a tectono-structural reorganization of the crater interior. The dip angle of these layers (measured at approximately 3°-4°) supports the hypothesis of an upward push consistent with a localized magmatic doming event. This doming, potentially caused by the intrusion of magmatic material into the subsurface, is also suggested by the reduced depth of the crater compared to similar nearby structures, and by the presence of an exposed rocky unit (Roc). The Roc unit is characterized by high apparent competence, blocky texture, and limited evidence of sedimentary reworking, which are consistent with a lithified substrate. These morphological properties are compatible with a volcanic or intrusive origin.

This uplift and tilting event may have fractured and displaced a pre-existing, stratified sedimentary or impact-derived fill unit originally covering the crater floor. Remnants of this unit are still preserved atop the tilted mesas in the north (Mes unit), as well as in the southern and western

sectors where the floor appears unaffected by doming (Lay unit). Concomitant or subsequent to the doming event, the intrusion of extensional tectonics associated with the Sirenum Fossae likely contributed to the fracturing and segmentation of the floor. In fact, the structural elements, particularly the fracture network within the crater floor, exhibit a strong alignment with regional tectonic features such as the Sirenum Fossae. This correlation suggests a broader structural control on the deformation observed within the crater, which is further evidenced by the tilted mesas and the presence of deep-seated gravitational slope deformations (DSGSDs) along the inner walls. In the terrestrial context, the DSGSDs are a particular category of large size mass movements, generally slow, that are often controlled by the inherited structural framework and affect entire mountain slopes with high relief energy. These deformations are particularly evident in the mesas, where elongated concave structures, like trenches, are observed.
Following these major geological events, impact into a volatile-rich substrate, tectonic intrusion by Sirenum Fossae, and magmatic doming, the crater entered a prolonged phase of surface modification during the Amazonian. This phase is dominated by periglacial and cryonival processes, which further altered the landscape without substantially modifying the primary geological framework. Features such as pingo-like mounds, polygonal terrain, and block fields are the result of ice-related surface dynamics acting upon the previously deformed and uplifted floor materials. These landforms record the final reshaping stage of the crater's evolution, characterized by freeze-thaw cycles, subsurface ice mobilization, and local mass wasting processes.
The observed landforms provide crucial evidence for the past and present surface dynamics within the crater. The presence of protalus rampart-like features (Hedding et al., 2010, Hauber et al., 2011) suggests the degradation of a once-extensive latitude-dependent mantle (LDM), reinforcing the notion that periglacial processes played a role in modifying the landscape. Latitude Dependent Mantle (LDM) is a layer composed of sand, dust, and rocks that are cemented by water ice, that covers at least 23% of martian surface (Kreslavsky & Head, 2002) and can be seen interacting with various surface features such as impact craters. Its origin is not yet agreed upon, but one of the theories connects it to the process of airfall deposition of ice-covered dust grains, which may be related to Mars' obliquity changes (Laskar et al., 2004) and those likely had a significant influence in a global circulation of water. Additionally, the identification of polygonal terrains, pingo-like structures, and block fields further supports the involvement of ice-related mechanisms. In the Martian context, polygonal terrains are generally classified based on their size and morphology (Levy et al., 2009). The observed polygons fall within the S1 category, characterized by small-scale fractures ranging from 10 to 50 meters in diameter, often forming orthogonal or random patterns. The formation of these polygons is typically associated with thermal contraction cracking in permafrost, further reinforcing the idea that ice was once, or still is, present in the subsurface.
On Earth, pingos are ice-cored mounds formed by the growth of ice lenses beneath the surface (Rowley et al., 2015), typically found in periglacial/crionival environments in presence of permafrost. Similar features have been observed on Mars at comparable latitudes (Dundas et al., 2008), further supporting the hypothesis that subsurface ice played a key role in shaping the crater's morphology. These structures are located on a relatively flat surface at the base of the northeastern wall and appear to be aligned along specific channels, possibly indicating preferential pathways for subsurface ice accumulation and mobilization.
The periglacial landforms include also the Block Fields, which are diffusely present throughout the crater, both on the tops of the inner walls and on the slopes of the central blocks. On Earth, the Block Fields are formed by the action of cryoclastism (Frost Weathering) caused by freeze-thaw cycles, which leads to the formation of angular block fields. Even in the Martian context they are probably generated by the same phenomenon. In fact, the formation zone of these angular boulders is clearly visible, their accumulation along the slope and in some cases their rolling due to gravity. The boulder trails could be in some cases mobilized by either the marsquakes or temperature/climate-controlled melting of ice (Roberts et al., 2012).

CONCLUSION

This study presents a detailed geomorphological map of Hala crater, a floor fractured crater located in the southern hemisphere of Mars, offering new insights into its surface morphology, unit distribution, and structural configuration. The high-resolution mapping which allowed the identification of the photogeological units, coupled with observed landforms such as polygonal terrains, pingo-like structures, gullies, and RSL, highlights the complexity of the crater's post-impact evolution. The crater presents rampart ejecta, which is indicative of a possible impact in volatiles rich terrains. The variations in topography, including the highest-standing knobs in the central and southern portion of the crater floor, could be connected to localized doming processes, possibly linked with the presence of the Sirenum Fossae graben. Structural mapping has further revealed alignments with the Sirenum Fossae system, indicating the influence of regional tectonic activity in controlling the fracturing and deformation of the crater floor. One possible hypothesis involves a combination of scenarios, which

could explain the presence of volcanic material inside the crater which is identified as Rocky unit, the polygonal fracture which dissect the crater and the stratigraphy and topographic differences between the mesas. We propose the interaction of processes, which involves tectonic and volcanic events.

The presence of periglacial features suggests a history of ice-related modification during the Amazonian period.

The map serves as a critical reference for future investigations into subsurface ice stability, climate evolution, and the broader geological context of FFCs on Mars. To further refine our understanding of the crater's history and its relationship to the broader Eridania Planitia region, future investigations will focus on three key aspects. First, mineralogical analyses will provide insight into the composition of different units, helping to constrain past alteration processes and potential volcanic activity. Second, radar data will be used to detect and map subsurface ice deposits, shedding light on past and present cryospheric conditions. Finally, crater dating techniques will establish a more precise chronological framework, enabling a better understanding of the temporal relationships between impact processes, tectonic activity, and ice-related modifications.

AUTHORS CONTRIBUTIONS:

SB: Investigation, Resources, Writing -Original Draft, Visualization, Mapping
MM: Conceptualization, Investigation, Validation, Writing – review and editing, Supervision
MCS: Conceptualization, Investigation, Validation, Writing – review and editing, Supervision
CB: Conceptualization, Investigation, Validation, Writing – review and editing, Supervision
GC: Writing – review and editing, Supervision, Project administration, Funding acquisition
MP: Validation, Writing – review and editing, Supervision
EH: Validation, Writing – review and editing, Supervision
GM: Resources, Writing – review and editing
AT: Resources, Writing – review and editing

ACKNOWLEDGEMENTS

This work has been developed under the ASI-INAF agreement n. 2024-40-HH.0 and in the framework of the "SPaceItUp Project" funded by ASI (Italian Space Agency) and by MUR (Ministry of University and Research), under contract n. 2024-5-E.0 - CUP n. I53D24000060005.

REFERENCES

Adeli S., Hauber E., Le Deit L., Jaumann R. (2015) - Geologic evolution of the eastern Eridania basin: implications for aqueous processes in the southern highlands of Mars. J. Geophys. Res. Planets, 120, 1774-1799, https://doi.org/10.1002/2015JE004898.

Agliardi F. & Crippa C. (2022) - Deep-Seated Gravitational Slope Deformations. Treatise on Geomorphology, 5, 183-199, https://dx.doi.org/10.1016/B978-0-12-818234-5.00182-6.

Balme M., Berman D.C., Bourke M.C., Zimberlman J.R. (2008) - Transverse Aeolian Ridges (TARs) on Mars. Geomorphology, 101, 703-720, https://doi.org/10.1016/j.geomorph.2008.03.011

Bamberg M., Jaumann R., Asche H., Kneissl T., Michael G.G. (2014) – Floor-Fractured Craters on Mars – Observations and Origin. Planetary and Space Science, 98, 146-162, https://doi.org/10.1016/j.pss.2013.09.017.

Barlow N. (2008) - Mars, an introduction to its interior, surface, and atmosphere. Cambridge University Press.

Bertoli S., Salvatore M.C., Pacifici A., Baroni C. (2024) - Geomorphological and Photogeological Units Map of Cilaos Crater: interpretation of landforms and surface processes in Eastern Promethei Terra, Mars. Geogr. Fis. Din. Quat., 47(2), 329-348, https://doi.org/10.4454/gtr56snb.

Bögli A 1960 - Kalklösung und Karrenbildung. Zeitsch. f. Geomorph. N. E. (2), 4-21.

Buczkowski D. L., Sizemore H. G., Bland M. T., Scully J. E. C., Quick L. C., Hughson K. H. G., Park R. S., Preusker F., Raymond C. A., Russell C. T. (2018) - Floor-Fractured Craters on Ceres and Implications for Interior Processes. J. Geophys. Res.: Planets, 123(12), 3188- 3204, https://doi.org/10.1029/2018JE005632.

Campobasso C., Carton A., Chelli A., D'Orefice M., Dramis F., Graciotti F., Guida D., Pambianchi G., Peduto F., and Pellegrini L. (2018) - Aggiornamento ed integrazioni delle linee guida della carta geomorfologica d'Italia alla scala 1: 50.000. Progetto CARG Quaderni serie III, 13, 15–26.

Capitan R.D. & Van De Wiel M. (2011) - Landform hierarchy and evolution in Gorgonum and Atlantis basins, Mars. Icarus, 211 (1), 366-388, https://doi.org/10.1016/j.icarus.2010.08.006

Carr M.H., Crumpler L.S., Cutts J.A., Greeley R., Guest J.E., and Masursky H. (1977) - Martian impact craters and emplacement of ejecta by surface flow, J. Geophys. Res., 82(28), 4055-4065, https://doi.org/10.1029/JS082i028p04055.

Della Seta M., Esposito C., Marmoni G.M., Martino S., Scarascia Mugnozza G., Troiani F. (2017) - Morpho-structural evolution of the valley-slope systems and related implications on slope-scale gravitational processes: New results from the Mt. Genzana case history (Central Apennines, Italy). Geomorphology, 289, 60-77, https://doi.org/10.1016/j.geomorph.2016.07.003.

Dramis F. & Sorriso-Valvo M. (1994) - Deep-Seated Gravitational Slope Deformations, Related Landslides and Tectonics. Engineering Geology, 38, 231-243, https://doi.org/10.1016/0013-7952(94)90040-X.

Dundas C.M. & McEwen A.S. (2010) - An assessment of evidence for pingos on Mars using HiRISE. Icarus, 205, 244-258, https://doi.org/10.1016/j.icarus.2009.02.020.

Grant J.A., Wilson S.A., Dobrea E.N., Fergason R.L., Griffes J.L., Moore J.M., Howard A.D. (2010) - HiRISE views enigmatic deposits in the Sirenum Fossae region of Mars. Icarus, 205, 53-63, https://doi.org/10.1016/j.icarus.2009.04.009.

Hanna J.C. & Phillips R.J. (2006) - Tectonic pressurization of aquifers in the formation of Mangala and Athabasca Valles, Mars. J. Geophys. Res., 111, https://doi.org/10.1029/2005JE002546.

Hartmann W.K. and Neukum G. (2001) - Cratering chronology and the evolution of Mars. In R. Kallenbach, J. Geiss, & W. K. Hartmann (Eds.), Chronology and evolution of Mars. Space sciences series of ISSI. Dordrecht: Springer, https://doi.org/10.1023/A:1011945222010.

Hauber E., Reiss D., Ulrich M., Preusker F., Trauthan F., Zanetti M., Hiesinger H., Jaumann R., Johansson L., Johnsson A., Van Gasselt S., Olvmo M. (2011) - Landscape evolution in Martian mid-latitude regions: insights from analogous periglacial landforms in Svalbard. Geological Society, London, Special Publications.

Hedding D.W., Meiklejohn K.I., Le Roux J.J., Loubser M. and Davis J.K. (2010) - Some observations on the formation of an active pronival rampart at Grunehogna Peaks, Western Dronning Maud Land, Antarctica. Permafrost Periglac. Process., 21, 355-361, https://doi.org/10.1002/ppp.698.

Hiesinger H., Head J.W. (2000) - Characteristics and origin of polygonal terrain in southern Utopia Planitia, Mars: results from Mars Orbiter Laser Altimeter and Mars Orbiter Camera Data. J. Geophys. Res., 105, 11999-12021., https://doi.org/10.1029/1999JE001193.

Howard A.D. and Moore J.M. (2004) - Scarp-bounded benches in Gorgonum Chaos, Mars: formed beneath an ice-covered lake? Geophys. Res. Lett., 31, L01702, https://doi.org/10.1029/2003GL018925.

Hubbard B., Milliken R. E., Kargel J. S., Limaye A., Souness C. (2011) - Geormorphological characterisation and interpretation of a mid-latitude glacier-like form: Hellas Planitia, Mars. Icarus, 211, 330-346, https://doi.org/10.1016/j.icarus.2010.10.021.

Irwin R.P.III, Howard A.D., and Maxwell T.A. (2004) - Geomorphology of Ma'adim Vallis, Mars, and associated paleolake basins. J. Geophys. Res., 109, E12009, https://doi.org/10.1029/2004JE002287.

Ivanov B.A. (2001) - Mars/Moon Cratering Rate Ratio Estimates. Space Science Reviews, 96, 87-104, https://doi.org/10.1023/A:1011941121102.

Jaumann R., Neukum G., Behnke T., Duxbury T.C. , Eichentopf K., Flohrer J., Gasselt S.v., Giese B., Gwinner K., Hauber E., Hoffmann H., Hoffmeister A., Köhler U., Matz K.-D., McCord T.B., Mertens V., Oberst J., Pischel R., Reiss D., Ress E., Roatsch T., Saiger P., Scholten F., Schwarz G., Stephan K., Wählisch M., the HRSC Co-Investigator Team 1 (2007) - The high-resolution stereo camera (HRSC) experiment on Mars Express: Instrument aspects and experiment conduct from interplanetary cruise through the nominal mission. Planet. Space Sci., 55, 928-952, https://doi.org/10.1016/j.pss.2006.12.003.

Jozwiak L.M., Head J.W., Neumann G.A., Zuber M.T., Smith D.E. (2012) - Lunar floor-fractured craters: classification, distribution, and implications for magmatism and shallow crustal structure. In: Lunar and Planetary Institute Science Conference Abstracts, 1512.

Komatsu G., Ori G.G, Di Lorenzo S., Rossi A.P., Neukum G. (2007) - Combinations of processes responsible for Martian impact crater "layered ejecta structures" emplacement. J. Geophys. Res., 112, E06005, https://doi.org/10.1029/2006JE002787.

Korteniemi J., Aittola M., Lahtela H., Ohman T., Raitala J. (2006) - Martian Floor-fractured Craters vs. Craters with Irregular Depressions. 37th Annual Lunar and Planetary Science Conference, March 13-17, 2006, League City, Texas, abstract no.2145.

Kreslavsky M., Head J.W. (2002) - Mars: Nature and evolution of young latitude-dependent water-ice-rich mantle. Geophys. Res. Lett., 29(15), https://doi.org/10.1029/2002GL015392.

Laskar J., Correia A.C.M., Gastineau M., Joutel F., Levrard B., Robutel P. (2004) - Long term evolution and chaotic diffusion of the insolation quantities of Mars. Icarus, 170, 343-364, https://doi.org/10.1016/j.icarus.2004.04.005.

Levy J., Head J. and Marchant D. (2009) - Thermal contraction crack polygons on Mars: Classification, distribution, and climate implications from HiRISE observations. J. Geophys. Res., 114, https://doi.org/10.1029/2008JE003273.

Luzzi E., Rossi A.P., Massironi M., Pozzobon R., Corti G., Maestrelli D. (2021) - Caldera Collapse as the Trigger of Chaos and Fractured Craters on the Moon and Mars. Geophys. Res. Lett., 48(11), https://doi.org/10.1029/2021GL092436.

Malin M.C., Bell III J. F., Cantor B.A., Caplinger M.A., Calvin W.M., Clancy R.T., Edgett K.S., Edwards L., Haberle R.M., James P.B., Lee S.W., Ravine M.A., Thomas P.C., Wolff M.J. (2007) - Context Camera Investigation on board the Mars Reconnaissance Orbiter. J. Geophys. Res., 112, E05S04, https://doi.org/10.1029/2006JE002808.

McEwen A.S., Eliason E.M., Bergstrom J.W., Bridges N.T., Hansen C.J., Delamere W.A., Grant J.A., Gulick V.C., Herkenhoff K.E., Keszthelyi L., Kirk R.L., Mellon M.T., Squyres S.W., Thomas N. & Weitz C.M. (2007) - Mars Reconnaissance Orbiter's High Resolution Imaging Science Experiment (HiRISE). J. Geophys. Res., 112, E05S02, https://doi.org/10.1029/2005JE002605.

McEwen A.S., Ojha L., Dundas C.M., Mattson S.S., Byrne S., Wray J.J., Cull S.C., Murchie S.L., Thomas N., Gulick V.C. (2011) - Seasonal flows on warm Martian Slopes. Science, 333, 740-743, https://doi.org/10.1126/science.1204816.

Mellon M.T., Feldman W.C. and Prettyman T.H. (2004) - The presence and stability of ground ice in the Southern hemisphere of Mars. Icarus, 169(2), 324-340, https://doi.org/10.1016/j.icarus.2003.10.022.

Mellon M.T., Arvidson R.E., Marlow J.J., Phillips R.J., Asphaug E. (2008) - Periglacial landforms at the Phoenix landing site and the northern plains of Mars. JGR: Planets, 113. https://doi.org/10.1029/2007JE003039.

Michalski J., Dobrea E., Niles P., Cuadros J. (2017) - Ancient hydrothermal seafloor deposits in Eridania basin on Mars. Nat. Commun., 8, 15978, https://doi.org/10.1038/ncomms15978.

Montigny A., Walwer D. and Michaut C. (2022) - The origin of hierarchical cracks in floor-fractured craters on Mars and the Moon. Earth Planet. Sci. Lett., 600, https://doi.org/10.1016/j.epsl.2022.117887.

Morris E.C., Underwood J.R. (1978) - Polygonal fractures of the Martian plains. Reports of Planetary Geology Program, 1977-1978, 97-99.

Mouginis-Mark P. (1979) - Martian fluidized crater morphology: Variations with crater size, latitude, altitude, and target material. J. Geophys. Res., 84, 8011-8022, https://doi.org/10.1029/JB084iB14p08011.

Osterloo M.M., Anderson F.S., Hamilton V.E., Hynek B.M. (2010) - Geologic context of proposed chloride-bearing materials on Mars. Journal of Geophysical Research (Planets), 115. https://doi.org/10.1029/2010JE003613

Pajola M., Rossato S., Carter J., Baratti E., Pozzobon R., Erculiani M.S., Corradini M., McBride K. (2016b) - Eridania Basin: An ancient paleolake floor as the next landing site for the Mars 2020 rover. Icarus, 275 (11), https://doi.org/10.1016/j.icarus.2016.03.029.

Pánek T. and Klimeš J. (2017) - Temporal behavior of deep-seated gravitational slope deformations: A review. Earth-Sci. Rev., 156, 14-38, https://doi.org/10.1016/j.earscirev.2016.02.007.

Pechmann J.C. (1980) - The origin of polygonal troughs on the northern plains of Mars Icarus, 185-210, https://doi.org/10.1016/0019-1035(80)90071-8.

Plug L.J. and Werner B.T., (2001) - Fracture networks in frozen ground. Journal of Geophysical Research, 106 (B5), 8599-8613, https://doi.org/10.1029/2000JB900320.

Roberts G.P., Matthews B., Bristow C., Guerrieri L., Vetterlein J. (2012) - Possible evidence of paleomarsquakes from fallen boulder populations, Cerberus Fossae, Mars. JGR Planets, 117(E2), https://doi.org/10.1029/2011JE003816.

Rowley T., Giardino J.R., Granados-Aguilar R. and Vitek J.D. (2015) – Periglacial processes and landforms in the critical zone. Dev. Earth Surf. Process., 19, 397-447, https://doi.org/10.1016/B978-0-444-63369-9.00013-6.

Sato H., Kurita K., Baratoux D. (2010) - The formation of floor-fractured craters in Xanthe Terra Icarus, 207, 248-264, https://doi.org/10.1016/j.icarus.2009.10.023.

Schultz P.H. (1976) - Floor-fractured lunar craters. The Moon, 15, 241-273, https://doi.org/10.1007/BF00562240.

Schultz P.H. and Gault D.E. (1979) - Atmospheric effects on Martian Ejecta Emplacement. J. Geophys. Res., 84, 7669-7687, https://doi.org/10.1029/JB084iB13p07669.

Smrekar S.E., McGill G.E., Raymond C.A., Dimitriou A.M. (2004) - Geologic evolution of the Martian dichotomy in the Ismenius area of Mars and implications for plains magnetization. J. Geophys. Res. (Planets), 109, 11002, https://doi.org/10.1029/2004JE002260.

Thomas N., Cremonese G., Ziethe R. et al. (2017) - The Colour and Stereo Surface Imaging System (CaSSIS) for the ExoMars Trace Gas Orbiter. Space Sci. Rev., 212, 1897-1944, https://doi.org/10.1007/s11214-017-0421-1.

Walwer D., Michaut C., Pinel V., Adda-Bedia M. (2021) - Magma ascent and emplacement below floor fractured craters on the Moon from floor uplift and fracture length. Phys. Earth Planet. Inter., 312, https://doi.org/10.1016/j.pepi.2021.106658.

Wendt L., Bishop J.L. and Neukum G. (2013) - Knob fields in the Terra Cimmeria/Terra Sirenum region of Mars: Stratigraphy, mineralogy, and morphology. Icarus, 225, 200-215, https://doi.org/10.1016/j.icarus.2013.03.020.

Wessel P., Luis J., Uleda L., Scharroo R., Wobbe F., Smith W.HF., Tiam D. (2019) - The Generic Mapping Tools Version 6. Geochem. Geophys. Geosyst., 20, 5556-5564. https://doi.org/10.1029/2019GC008515.

Wichman R.W and Schultz P.H. (1996) - Crater-centered laccoliths on the moon: modeling intrusion depth and magmatic pressure at the crater taruntius. Icarus, 122, 193-199. https://doi.org/10.1006/icar.1996.0118

Wilson L. and Head III J.W. (2002) - Tharsis-radial graben systems as the surface manifestation of plume-related dike intrusion complexes: Models and implications. J. Geophys. Res., 107(E8). https://doi.org/10.1029/2001JE001593

Zegers T.E., Oosthoek J.H.P., Rossi A.P., Blom J.K., Schumacher S. (2010) - Melt and collapse of buried water ice: an alternative hypothesis for the formation of chaotic terrains on Mars Earth Planet. Sci. Lett., 297, 496-504, https://doi.org/10.1016/j.epsl.2010.06.049.

Manuscript received 24 July 2025; accepted 16 February 2026; published online XX March 2026;
editorial responsibility and handling by V. Galluzzi.